Author/s:
Korasidis, VA;Wing, SL;Shields, CA;Kiehl, JT

Title:
Global Changes in Terrestrial Vegetation and Continental Climate During the Paleocene-Eocene Thermal Maximum

Date:
2022-04-01

Citation:
Korasidis, V. A., Wing, S. L., Shields, C. A. & Kiehl, J. T. (2022). Global Changes in Terrestrial Vegetation and Continental Climate During the Paleocene-Eocene Thermal Maximum. Paleoceanography and Paleoclimatology, 37 (4), https://doi.org/10.1029/2021PA004325.

Persistent Link:
https://hdl.handle.net/11343/308240

Paleoceanography and Paleoclimatology

RESEARCH ARTICLE
10.1029/2021PA004325

Special Section:
DeepMIP in the Hothouse Earth: late Paleocene - early Eocene climates and their lessons for the future

Global Changes in Terrestrial Vegetation and Continental Climate During the Paleocene-Eocene Thermal Maximum

Vera A. Korasidis[1,2], Scott L. Wing[1], Christine A. Shields[3], and Jeffrey T. Kiehl[4]

[1]Department of Paleobiology, National Museum of Natural History, Smithsonian Institution, Washington, DC, USA, [2]School of Geography, Earth and Atmospheric Sciences, University of Melbourne, Parkville, VIC, Australia, [3]National Center for Atmospheric Research, Boulder, CO, USA, [4]University of California, Santa Cruz, Santa Cruz, CA, USA

Key Points:

- We assess how terrestrial vegetation and climate changed globally during the Paleocene-Eocene Thermal Maximum (PETM) using published records of spores and pollen
- Palynofloral data and models agree on the expansion poleward of temperate and tropical climates at high and middle latitudes during the PETM
- Proxy reconstructions are generally warmer at high latitudes and in mid-latitude continental interiors, particularly in the pre-PETM

Supporting Information:

Supporting Information may be found in the online version of this article.

Correspondence to:

V. A. Korasidis,
korasidisv@si.edu

Citation:

Korasidis, V. A., Wing, S. L., Shields, C. A., & Kiehl, J. T. (2022). Global changes in terrestrial vegetation and continental climate during the Paleocene-Eocene Thermal Maximum. *Paleoceanography and Paleoclimatology*, *37*, e2021PA004325. https://doi.org/10.1029/2021PA004325

Received 18 JUN 2021
Accepted 4 APR 2022

Abstract Most studies of the response of terrestrial vegetation to climate change during the Paleocene-Eocene Thermal Maximum (PETM) have focused on individual sites and sections. To get a broader perspective we compiled published records of terrestrial pollen and spores across the Paleocene-Eocene transition at 38 sites around the globe. For the 10 sites with quantitative data PETM palynofloras were largely distinct in composition from those in the latest Paleocene or post-PETM early Eocene. We also inferred paleoclimatic conditions at each site from the distributions of nearest living relatives (NLRs) of fossil pollen taxa among present-day Köppen climate types. The NLRs of Paleocene high-paleolatitude palynotaxa are most diverse in cooler climates, whereas the NLRs of PETM taxa are more diverse in warmer, wetter climates. At middle-paleolatitudes NLRs of Paleocene palynotaxa are most diverse in warm, wet climates, whereas NLRs of PETM palynotaxa are most diverse in warm, seasonally dry climates. In the tropics there is little change from Paleocene to PETM in the climate distributions of NLRs. We compared changes in paleoclimate reconstructed from the Köppen distributions of the NLRs with those simulated from the Community Earth System Model (version CESM1.2). Paleoclimatic changes during the PETM inferred from palynological proxies are mostly consistent with modeled climate changes, including the expansion of temperate climates at the expense of cold climate types at high-paleolatitudes and the expansion of temperate and tropical climates in middle-paleolatitudes. Despite this concordance, modeled winter temperatures in continental interiors and high-paleolatitudes remain colder than those reconstructed from NLR distributions.

1. Introduction

During the Paleocene-Eocene Thermal Maximum (PETM, ~56 Ma) a massive release of isotopically light carbon to the ocean-atmosphere system generated a large negative carbon isotope excursion (CIE) and global warming of 4–8°C (Dickens et al., 1995, 1997; Jones et al., 2013; Kennett & Stott, 1991; McInerney & Wing, 2011). The PETM is known best from marine records, but disparate lines of geochemical, sedimentological and paleobiological evidence suggest there was accompanying paleoclimatic change on the continents, including increases in temperature and higher rates of precipitation and erosion (summarized in Carmichael et al., 2017, 2018; Hollis et al., 2019). Existing evidence also suggests geographically heterogeneous responses to the event. High-paleolatitudes became warmer and experienced stable or increasing rainfall, whereas mid-to-low paleolatitudes and continental interiors became warmer and experienced either decreasing precipitation or increasingly episodic or extreme precipitation events (Carmichael et al., 2017, 2018; Hollis et al., 2019). Model results also predict higher temperatures and higher frequency of intense precipitation events during the PETM than in the preceding late Paleocene, especially at low to middle paleolatitudes (Carmichael et al., 2018; Kiehl et al., 2018; Rush et al., 2021; Shields et al., 2021).

The purpose of this study is to bring together for the first time all published records of terrestrial spore and pollen change across the PETM to develop the broadest geographic understanding of how terrestrial vegetation and climate changed during the event. The composition and structure of terrestrial vegetation is a sensitive index of climate, or to quote Köppen and Geiger (1936) vegetation is "…crystallized, visible climate in which many features are more evident than in the information provided by our instruments". Similarly fossil plants should be a sensitive index of many aspects of paleoclimatic change.

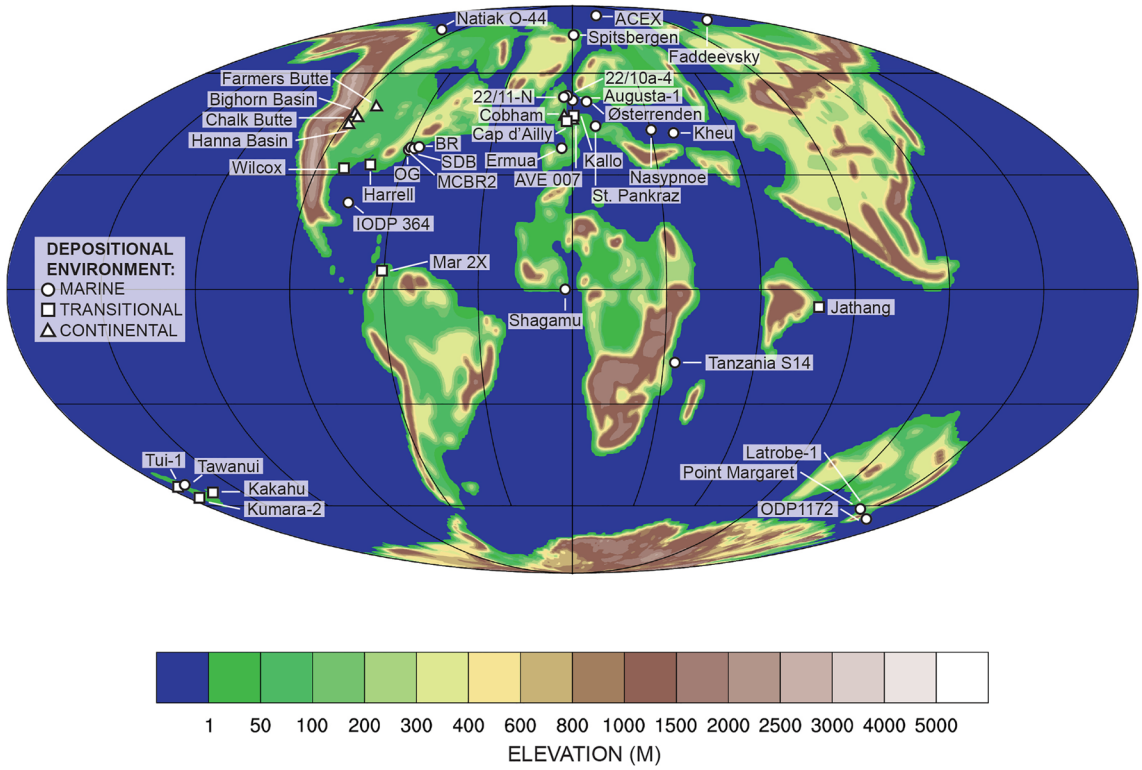

Figure 1. Global paleogeographic reconstruction for 56 Ma illustrating the positions and general depositional settings of PETM palynofloral sites. Paleogeographic positions and paleotopography (in meters) from Herold et al. (2014). For additional details regarding the paleogeographic positions, palynofloral sites and depositional environments refer to Table S1.

2. Methodology

Palynofloral records from 38 sites have been included in this study (Figure 1). The confidence with which these sections can be correlated to the PETM varies, but most display either the characteristic CIE or are correlated to the Paleocene-Eocene boundary through regional and/or global biostratigraphic constraints. All sites are here classified as either continental, transitional or marine based on sedimentological and paleontological features described in the original papers (Table S1). Following Tschudy (1969) fluvial, lacustrine, palustrine, swamp/marsh and paleosol sediments are classified as continental deposits; deltaic (i.e., delta plain, pro-delta), coastal marsh, lagoonal, littoral, coastal plain and near-shore marine sediments as transitional deposits; and neritic (shallow marine/continental shelf), bathyal (continental slope), abyssal (fully to deep marine) and restricted marine sediments as marine deposits. In this study, sites situated above 60° north and south of the equator at the time of deposition are classified as high paleolatitude, between 60° and 30° north and south of the equator as middle paleolatitude and between 30° north and south of the equator as low paleolatitude.

2.1. Palynofloral Abundance Data

Ten of the studies published raw palynological counts and/or relative-abundance data for genus or species-level taxa and are correlated to the PETM through a minimum of two independent proxies (Table S2). In some sections, the PETM was divided into three phases: the rapid onset defined by a −4 to −5‰ CIE, a ∼100 ky-long CIE "body" with stable negative carbon isotope composition, and an ∼80 ky recovery period during which carbon isotope values returned to pre-onset levels (Bowen et al., 2006; Westerhold et al., 2018). We honor the assignment of samples to the "body" or "recovery" phase of the CIE if designated in the original studies. For the non-metric dimensional scaling (NMDS) analysis, every sample of late Paleocene, PETM or post-PETM early Eocene age was included except for the long Mar 2X site record for which we focused on the interval from ∼170 to 400 m to remove much older and younger samples. Due to the differences in sample sizes, sporomorph percentages were used as input for the ordination analyses, and only samples with counts >50 individual grains were evaluated.

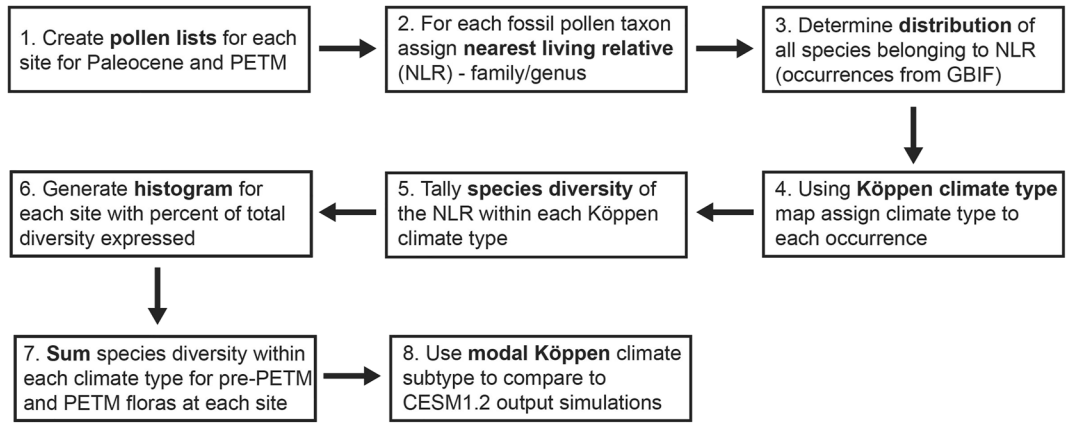

Figure 2. Summary of steps undertaken to generate palynofloral-based Köppen climate type estimates for pre-PETM and PETM floras at each site.

Pairwise Bray-Curtis distances were calculated between samples in each section and used in non-metric multidimensional scaling (NMDS) ordinations performed with the ecodist package version 2.0.1 in R version 1.1.5001.

2.2. Inferring Köppen Climate Types From Palynofloras

To reconstruct climatic change across the PETM from pollen and spores we have used the nearest living relative (NLR) approach, which infers paleoclimate from fossil plants based on the climatic ranges of their present-day living relatives. The NLR approach has been used for more than 150 years (Heer, 1870), the underlying assumptions have been widely discussed, and many variants have been developed (e.g., Berry, 1930; Grimm & Denk, 2012; Harbert & Nixon, 2015; Peppe et al., 2018; Reichgelt et al., 2018; Tiffney, 1994; Utescher et al., 2014; Wing & Greenwood, 1993; Wolfe, 1971). For pollen and spore assemblages some version of the NLR approach is the only method available for extracting paleoclimate information because there are no recognized morphological correlates between sporomorph form and climate.

The correct identification of fossil plants is critical to making reliable paleoclimate inferences from the distributions of their living relatives. For Paleogene pollen and spores there is a range of opinions regarding how precisely they can be identified taxonomically. Some authors assign many dispersed Paleogene sporomorphs to extant genera (e.g., Suan et al., 2017; Suc et al., 2020). Identification at the generic level or below yields NLR clades with fewer living species that therefore have a more restricted climatic envelope and thus suggest more specific paleoclimatic conditions. Other authors use a combination of characters visible in light and electron microscopy to assign Paleogene sporomorphs to a variety of taxonomic levels depending on how diagnostic their features are (e.g., Bouchal et al., 2014; Grímsson et al., 2015; Manchester et al., 2015). Paleoclimatic inferences thus have intermediate specificity depending on the particular fossil taxa in the assemblage and how narrowly they can be circumscribed taxonomically. Palynological biostratigraphers have historically aimed to identify palynomorphs using light microscopy alone and have identified fossil taxa to well-established forms that are generally assigned to plant families but less often to extant genera (e.g., Willard et al., 2019). We have relied in this paper on identifications made by the original authors, most of whom adopted this last taxonomic approach.

Because most plant families or tribes are distributed across a broad range of climates, reliance on form taxa and higher taxa reduces the resolution of our paleoclimate inferences. There are two positive aspects to using higher taxa, though. First, some families of flowering plants have centers of diversity in specific climate types even though their species occur in many climates (Punyasena, 2008). Second, many Paleogene pollen types that strongly resemble extant genera belong to extinct genera when they are found in situ and characters of their flowers and leaves become known (e.g., Manchester & Dilcher, 1997; Manchester et al., 2004). The climatic distribution of the extant family may provide less specific but also less misleading paleoclimatic inferences if additional information shows the pollen does not actually belong to any living genus.

In this study, for each of the 10 sites with quantitative data we made two lists: all pollen and spore taxa present in the pre-PETM samples and all taxa present in the PETM samples (Figure 2). We focus on relative diversity of

taxa in the palynoflora rather than their relative abundance because abundance is likely to be influenced by many factors with little climatic significance including pollen production, preservation, transport, and deposition. We relied on the original authors' identifications and assignments to determine NLRs but updated the higher taxonomy where needed (see Table S3). The number and percentage of pre-PETM and PETM palynofloras with NLRs for each site is available in Table S4.

We searched the Global Biodiversity Information Facility at gbif.org on November 2 and 3, 2020, for all occurrences of living species belonging to each of the higher NLR taxa in the assimilated lists and downloaded the records. This data set represents an amalgamation of unbiased records from several publishing authorities and is available to download. We manually filtered out GBIF records that had imprecise coordinates (>1 km precision) or that had altitudes of ≤0 or >4000 m, reasoning that these were likely spurious or that the coordinates were derived from the centroids of political units.

We assigned each living species occurrence to a Köppen-Geiger climate type (Köppen & Geiger, 1936) using the gridded data set provided by Beck et al. (2018). The 0.0083° resolution (approximately 1 km at the equator) of this global map is much higher than that available in earlier versions (Kottek et al., 2006), which improves classification accuracy particularly in regions with sharp spatial and/or elevation gradients in climate. The climate data used by Beck et al. (2018) were explicitly corrected for topographic effects. We used the Köppen-Geiger system in preference to climate variables such as mean annual or monthly mean precipitation and temperature because they well express the interaction of climatic variables that are important in influencing vegetation (Denk et al., 2013). The Köppen-Geiger system defines five major climate types: tropical (A), dry (B), temperate (C), continental (D) and polar (E). 30 climate subtypes are defined using threshold values in the seasonality of temperature and precipitation in such a way that subtypes are usually dominated by one major vegetational type (Beck et al., 2018; Kottek et al., 2006). Critical values defining the boundaries of the climate types and subtypes are from (Beck et al., 2018; Table 1).

For each higher taxon we calculated the number of extant species occurring in each Köppen-Geiger climate subtype, removing climate subtypes present by virtue of a single occurrence because many of these were incorrectly located or were horticultural specimens. We then created a histogram for each higher taxon showing the number of its living species found in each Köppen-Geiger climate subtype—the diversity of the taxon in climate space. These taxon-specific distributions in Köppen-Geiger climate space were then summed and relativized for all the NLRs of the total pre-PETM and total PETM palynofloras at each of the 10 sites. We show the proportion of total NLR species diversity in each Köppen-Geiger subtype (Table S5) and consider the modal climate subtype to be the best estimate of the paleoclimate. We used the modal Köppen-Geiger climate subtype derived in this way to compare with Köppen-Geiger climate subtypes calculated from output of CESM 1.2 simulations, described in Section 2.3.

We did not search for occurrence data nor generate Köppen-Geiger climate distributions for extant species of Paleocene-Eocene higher taxa whose crown groups diversified greatly in the middle to late Cenozoic because these diverse recent radiations might be misleading about the climate preferences of stem relatives. Examples of families thought to have had strong post-PETM crown group diversification of mostly herbaceous lineages included Asteraceae (Mandel et al., 2019), Amaranthaceae (Kadereit et al., 2003), Convolvulaceae (Mitchell et al., 2016) and Myrtaceae (Thornhill et al., 2012). We also omitted higher taxa with present-day cosmopolitan distributions across all climate zones. This includes Euphorbiaceae (Webster, 1994) and Poaceae (Soreng et al., 2015) which underwent major mid- or late-Cenozoic crown group radiations in both tropical and temperate regions. For the complete list of excluded taxa see Table S6. An alternate approach in which the preferred climate of the Paleogene ancestors is reconstructed from chronograms of clades of interest is beyond the scope of the current study, especially because we have not been able to independently evaluate previously published identifications of Paleocene-Eocene palynomorphs.

2.3. CESM1.2 Simulations and Model Derived Köppen Data

The Community Earth System Model, Version 1.2 (CESM1.2) is a sophisticated Earth system modeling framework that can be applied to deep time paleoclimate periods such as the pre-PETM and PETM (Kiehl et al., 2021; Rush et al., 2021; Shields et al., 2021). Here, we employ a high-resolution (~0.25°) fixed sea surface temperature configuration with coupling between the atmosphere component, CAM5.3 (Community Atmosphere Model,

Table 1
Overview of the Köppen-Geiger Climate Classes Including the Defining Criteria From Beck et al. (2018)

1st	2nd	3rd	Description	Criterion
A			Tropical	Not (B) & $T_{cold} \geq 18$
	f		- Rainforest	$P_{dry} \geq 60$
	m		- Monsoon	Not (Af) & $P_{dry} \geq 100 - MAP/25$
	w		- Savannah	Not (Af) & $P_{dry} < 100 - MAP/25$
B			Arid	$MAP < 10 \times P_{threshold}$
	W		- Desert	$MAP < 5 \times P_{threshold}$
	S		- Steppe	$MAP \geq 5 \times P_{threshold}$
		h	- Hot	$MAT \geq 18$
		k	- Cold	$MAT < 18$
C			Temperate	Not (B) & $T_{hot} > 10$ & $0 < T_{cold} < 18$
	s		- Dry summer	$P_{sdry} < 40$ & $P_{sdry} < P_{wwet}/3$
	w		- Dry winter	$P_{wdry} < P_{swet}/10$
	f		- Without dry season	Not (Cs) or (Cw)
		a	- Hot summer	$Thot \geq 22$
		b	- Warm summer	Not (a) & $T_{mon}10 \geq 4$
		c	- Cold summer	Not (a or b) & $1 \leq T_{mon}10 < 4$
D			Cold	Not (B) & $T_{hot} > 10$ & $T_{cold} \leq 0$
	s		- Dry summer	$P_{sdry} < 40$ & $P_{sdry} < P_{wwet}/3$
	w		- Dry winter	$P_{wdry} < P_{swet}/10$
	f		- Without dry season	Not (Ds) or (Dw)
		a	- Hot summer	$T_{hot} \geq 22$
		b	- Warm summer	Not (a) & $T_{mon}10 \geq 4$
		c	- Cold summer	Not (a, b or d)
		d	- Very cold winter	Not (a or b) & $T_{cold} < -38$
E			Polar	Not (B) & $T_{hot} \leq 10$
	T		- Tundra	$T_{hot} > 0$
	F		- Frost	$T_{hot} \leq 0$

Note. Variable definitions: MAT = mean annual air temperature (°C); T_{cold} = the air temperature of the coldest month (°C); T_{hot} = the air temperature of the warmest month (°C); $T_{mon}10$ = the number of months with air temperature >10°C (unitless); MAP = mean annual precipitation (mm yr^{-1}); P_{dry} = precipitation in the driest month (mm $month^{-1}$); P_{sdry} = precipitation in the driest month in summer (mm $month^{-1}$); P_{wdry} = precipitation in the driest month in winter (mm $month^{-1}$); P_{swet} = precipitation in the wettest month in summer (mm $month^{-1}$); P_{wwet} = precipitation in the wettest month in winter (mm $month^{-1}$); $P_{threshold} = 2 \times MAT$ if >70% of precipitation falls in winter, $P_{threshold} = 2 \times MAT + 28$ if >70% of precipitation falls in summer, otherwise $P_{threshold} = 2 \times MAT + 14$. Summer (winter) is the 6-month period that is warmer (colder) between April-September and October-March.

Version 5.3), the land component, CLM4 (Community Land Model, Version 4), and the River Transport Model (RTM) (Lawrence et al., 2011; Neale et al., 2010; Park et al., 2014). RTM is executed independently from CLM4 and, because of uncertainties in the paleotopography, we simply utilize the standard 1° resolution. Sea surface temperatures are computed from equilibrated, lower resolution (~2°) fully-coupled companion simulations. The 2° fully-coupled runs were integrated for ~1800 years with the final 20 years used for the sea surface temperature climatology. Paleotopography, paleobathymetry, and PETM vegetation climate types are taken from the DeepMIP forcing datasets (Herold et al., 2014; Lunt et al., 2017) with solar and orbital forcings adopted from Kiehl et al. (2018). Given the potential influence of orbital configuration on seasonal precipitation patterns and intensity in the Northern Hemisphere (e.g., the monsoons) during the pre-PETM and PETM (Zeebe & Lourens, 2019), simulations include an orbital configuration that maximizes insolation for NH summers (Shields et al., 2021).

Table 2
Forcings and Model Simulation Across the Simulations Presented

Simulation	CO_2	CH_4	Solar	Orbit
PETM_Orbmax	1590 ppmv	16 ppmv	1355 W m^{-2}	Maximum NH
pre_PETM_Orbmax	680 ppmv	16 ppmv	1355 W m^{-2}	Maximum NH

Note. Greenhouse gases are in ppmv, solar forcing is in W m^{-2}, and the orbit is relative to the Northern Hemisphere (NH).

The maximum Northern Hemisphere orbit is applied with an obliquity of 24.5°, an eccentricity of 0.06, and a moving vernal equinox of 270°. Organic aerosol emissions for CAM5 were created using the MEGAN (Model of Emissions of Gases and Aerosols) module from CLM4.0 and approximated using PETM climate types (Guenther et al., 2012). We present two simulations with differing greenhouse gases, late Paleocene (pre-PETM) and the PETM, to evaluate the transition between these two periods. Table 2 details greenhouse gas levels, solar, and orbital obliquity for each simulation.

Monthly climatologies of surface air temperature and precipitation (including phase) are applied to the Köppen category algorithms found in Beck et al. (2018) and Kottek et al. (2006). High model fidelity Köppen categories are assigned to each grid point in the model domain used to create the maps found in the Results section. In addition, to account for the existence of climatic conditions in the Paleogene simulations that exceed modern temperature limits, any grid cells that surpass modern MATs (i.e., 31.4°C), as derived from Fick and Hijmans (2017), are assigned to Köppen categories but classified as "out of range" in the Results section. Grid point spacing is ~0.25°, which is approximately 25 km. We use the average climate type of the nine closest terrestrial grid cells to the palynofloral sites to estimate the Köppen climate type. For the transitional and marine sites, we selected coastal cells rather than inland cells to capture the sampling radius of typical lowland palynofloral assemblages.

3. Results

3.1. Palynofloral Composition

Most of the NMDS analyses show that palynofloral samples from the CIE body and recovery occupy a portion of the ordination plot distinct from both latest Paleocene and post-CIE Eocene samples (Figure 3). In the ACEX core, 22/11-N core and Bighorn Basin, samples from the latest Paleocene, CIE body, CIE recovery, and post-PETM Eocene occupy different parts of the NMDS ordinations. Samples from the CIE body at Harrell and Kumara-2 also occupy a distinctive portion of the ordination plot relative to the pre-PETM, and for Kumara-2, the PETM samples are distinct from the post-PETM Eocene as well. At Natiak O-44, ODP 1172 and Tawanui, the CIE body samples occupy a distinct portion of the ordination plot relative to the pre-PETM, but overlap with post-PETM Eocene samples. At Chalk Butte, the CIE body samples are distinct from post-PETM Eocene samples, but not from pre-PETM samples. At the Mar 2X site, samples from the pre-PETM, PETM and post-PETM early Eocene overlap broadly in composition.

3.2. Köppen Climate Types

We generated plots of the distributions of NLRs among Köppen climate types using the methods described above for the 10 sites with full palynofloral lists from both the pre-PETM and PETM (see Figure 4 for select examples and Figure S1 for all sites). In general, high paleolatitude pre-PETM sites are characterized by high proportions of fossil species with living relatives in the Cfa and Cfb climate types and moderate diversity in Dfb and Dfa climate types. In contrast, the middle latitude pre-PETM sites are characterized by high proportions of fossil species with living relatives in the Cfa and Cfb climate types and moderate diversity in the Am and Aw climate types. The low latitude pre-PETM sites are characterized by high proportions of fossil species with living relatives in the Af, Am and/or Aw climate types. Notably, across all paleolatitudes, the PETM coincides with an increase in the proportions of fossil species with living relatives in the Af, Am and/or Aw climate types (Figure 4).

In general, the model predicts that cold climate types (Dfa, Dfb, Dwa) dominated high paleolatitudes, temperate climate types (Cfa, Csa, Cwa) characterized middle paleolatitudes, while tropical climate types (i.e., Aw, Am

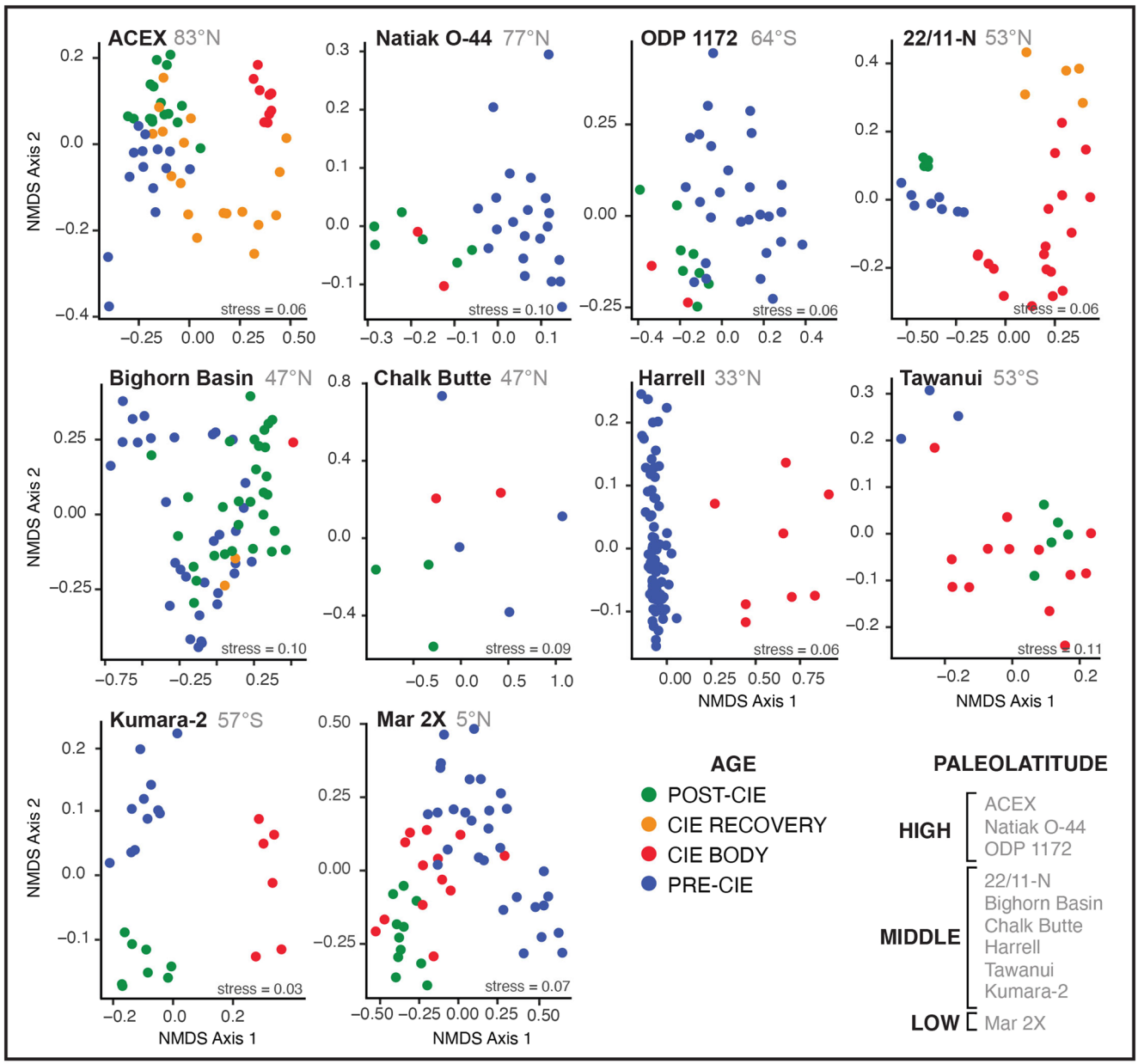

Figure 3. Change in the composition of terrestrial palynofloras across the Paleocene-Eocene transition. Each of the 10 graphs is a nonmetric multidimensional scaling analysis that summarizes published species-level relative abundance data for the samples at a site (S1, S4). Samples are coded as indicated in the key. At most sites, samples from the body of the CIE occupy a distinct region of the plot because their palynofloras are different in composition from the pre-PETM latest Paleocene and post-PETM early Eocene.

and Af) dominated low paleolatitudes in the pre-PETM, except for low latitude grid cells that were out of range (Figure 5).

For the proxy data sites the palynofloral-derived Köppen climate types at high paleolatitudes during the pre-PETM are temperate (i.e., Cfa and Cfb), whereas the model predicts cold climate types (i.e., Dfa and Dfb). Pre-PETM, Köppen climate types inferred from proxy data at middle paleolatitude sites suggest widespread temperate climates (i.e., Cfb). The model, however, predicts the proxy data sites would have had temperate (i.e., Cfa, Csa) or cold (i.e., Dfa) climate types during the pre-PETM. For the low paleolatitude Mar 2X site both the palynoflora and model predict a tropical Aw Köppen climate during the pre-PETM.

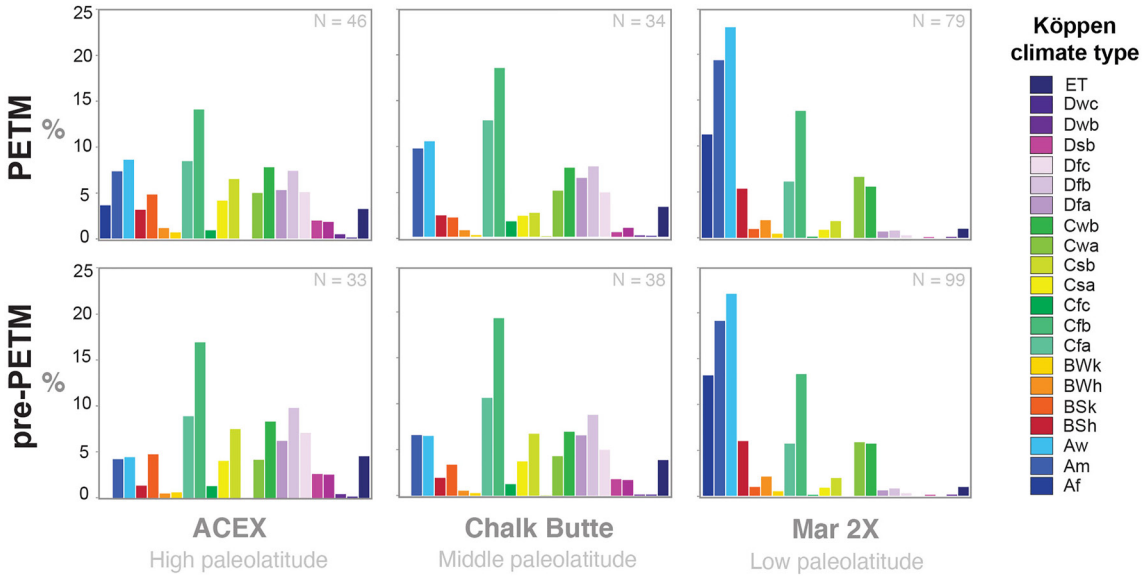

Figure 4. Köppen climate type distributions for select sites for the pre-PETM and PETM. The *y*-axis is the percent of all species of living relatives of the fossil in each climate type for palynofloras at each site represented as a percentage. "N" represents the number of living species with NLRs on which the percentage is based on (refer to Table S4 for additional information).

In general, the climate model predicts the co-dominance of cold (Dfa, Dfb, Dwa) and temperate (i.e., Cfa, Cfb, Cwa, Csa) climate types at high paleolatitudes during the PETM (Figure 6). In order of decreasing abundance, the model predicts temperate (Cwa, Csa, Cfa), tropical (Aw, Am, Af) and arid (BWh, BSh) climate types during the PETM in middle paleolatitudes. The model predicts the occurrence of tropical (i.e., Aw, Am, Af) and arid (i.e., BWh, BSh) types occurring in some low-latitude coastal regions, however the vast majority of low paleolatitudes exceed all modern climates in terms of temperature and are coded as out of range in Figure 6.

For high paleolatitude proxy sites we inferred Köppen climates in the temperate (i.e., Cfb) and cold (Dfb at the Natiak site only) categories during the PETM. The model predicts temperate (i.e., Cfa) and a broad area of cold climates (i.e., Dfa). Palynofloral-derived Köppen estimates from the middle paleolatitude sites suggest temperate climate types (i.e., Cfb) during the PETM. The model predicts mostly Cfa climate type for these sites, though for the Harrell core the model predicts a tropical (Aw) climate. The proxy estimate for the Mar 2X site during the

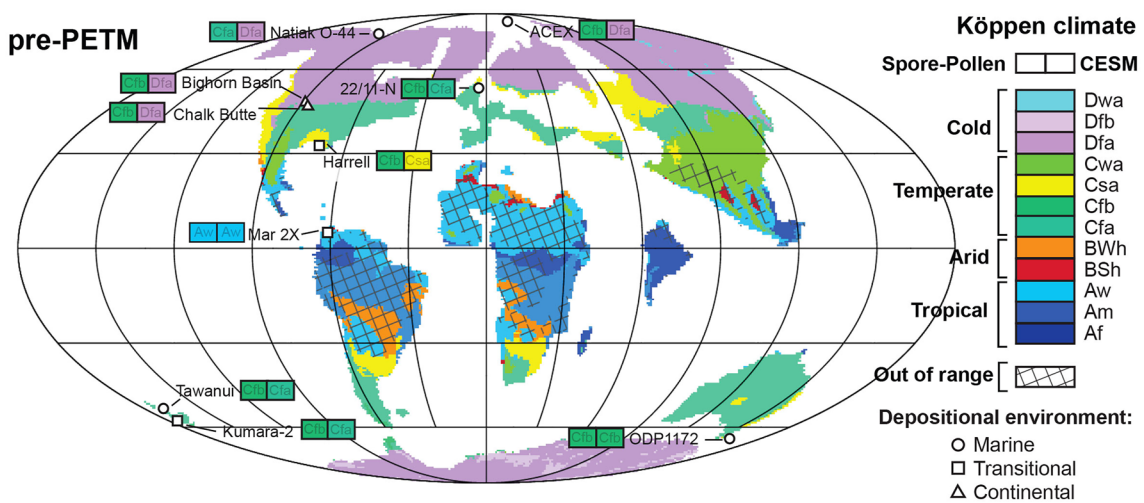

Figure 5. pre-PETM Köppen climate type simulations from the palynofloral-derived modal Köppen climate type for each site (left rectangle) and high resolution CESM 1.2 simulation for each site (right rectangle) and globally. The predicted Köppen climate type for each site represents the average climate type of the nine closest terrestrial grid cells. The CESM 1.2 simulation employs maximum orbital parameters.

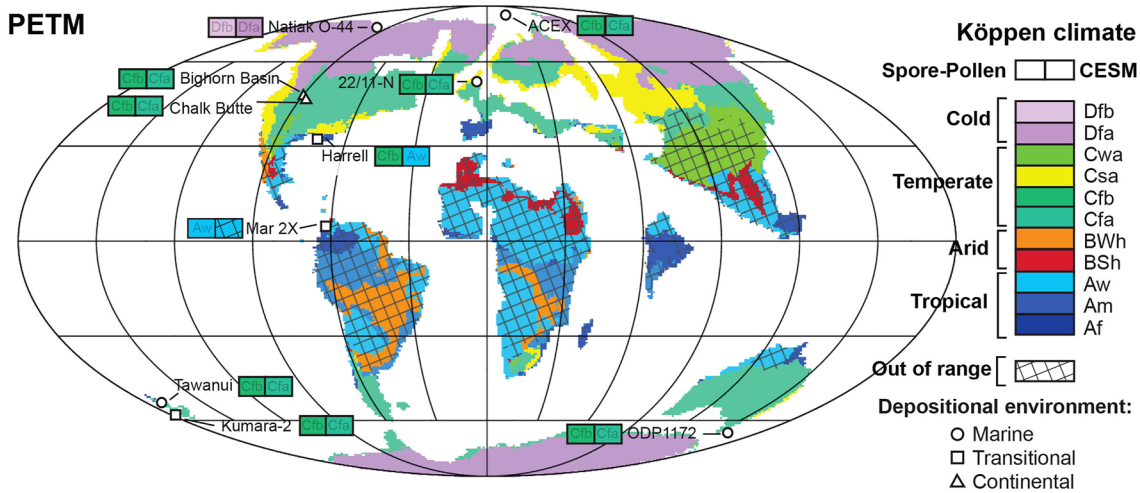

Figure 6. PETM Köppen climate type simulations from the palynofloral-derived modal Köppen climate type for each site (left rectangle) and high resolution CESM 1.2 simulation for each site (right rectangle) and globally. The predicted Köppen climate type for each site represents the average climate type of the nine closest terrestrial grid cells. The CESM 1.2 simulation employs maximum orbital parameters.

PETM is Aw, possibly reflecting the inability of the NLR method to predict climates hotter than modern ones, but the model predicts a climate that is out of range.

4. Discussion

4.1. Prominent and Widespread PETM Palynofloral Turnover

The floristic distinctiveness of PETM palynofloras at each site for which there is taxonomically differentiated data (Figure 3 and Table S7) suggests there were prominent changes in vegetation in response to the PETM across the Earth, albeit of different types in different places. At high northern paleolatitude sites (Table S7), palynofloral change included an increased abundance of Cupressaceae. This pollen probably derived from the genera *Metasequoia* and/or *Glyptostrobus* (Frederiksen, 1980; Pocknall, 1987), which are common as megafossils in peat and clastic swamp settings at middle and high latitudes during the Paleogene (e.g., McIver & Basinger, 1999; Richter & LePage, 2005). Living *Glyptostrobus pensilis* requires wet substrates (Averyanov et al., 2009). The increase in cupressaceous pollen likely suggests wetter substrates and higher precipitation during the PETM. The increased relative abundance of tropical and subtropical Arecaceae (palm) and Bombacoideae (silk cotton tree and relatives) pollen in the high paleolatitude ACEX core during the PETM is also indicative of a temperature increase (Eiserhardt et al., 2011; Linares-Palomino & Alvarez, 2005; Svenning et al., 2008). The decreased relative abundance of Pinaceae (conifer) pollen at three sites (McNeil et al., 2013; Suan et al., 2017; Willard et al., 2019) is also consistent with a temperature increase in high northern paleolatitudes because these pollen types were probably derived from conifers that grew under temperate and cooler conditions (Jagels & Equiza, 2005; McIver & Basinger, 1999). The distinctiveness of samples from the CIE body in the ACEX core (Figure 3) likely results from the increase in Cupressaceae, Arecaceae and Bombacoideae pollen and concurrent decrease in Pinaceae pollen abundance. The appearance of probable warm temperate lineages during the PETM in North America (i.e., the juglandaceous genus *Platycarya* and pollen similar to *Tilia* referred to as *Intratriporopollenites instructus;* Wing et al., 2005) also suggests high northern paleolatitudes had warm enough climates to permit establishment of populations of these lineages and longitudinal dispersal from Europe and/or Asia to North America.

In the southern high- latitudes, the rapid increase in abundance of Picrodendraceae (*Austrobuxus*/*Dissiliaria*; pink cherry; see Table S7), a group that is today most diverse in wet tropical rainforests (Airy Shaw, 1974; Forster, 1997; Tryon & Tryon, 2012), suggests enhanced precipitation from the pre-PETM to PETM. High abundances of *Wollemia* pollen at ODP site 1172 during the PETM are consistent with higher precipitation because this genus has a modern distribution in wet rainforests and was abundant during previous wet periods in Australasia such as the Turonian (Partridge, 2004; Fletcher et al., 2014; Vajda & McLoughlin, 2005). The increased relative abundance of tropical to subtropical Arecaceae (palm) and tropical *Nypa* (mangrove palm) pollen at

southern high-paleolatitude sites also indicates a temperature increase (Table S7; Baker & Couvreur, 2013; Eiserhardt et al., 2011; Reichgelt et al., 2018; Theerawitaya et al., 2014). The concurrent decline in Podocarpaceae (podocarp) pollen (Contreras et al., 2014; Huurdeman et al., 2021), common in cool-temperate climates during the Paleogene (Hill & Gibson, 1986; Macphail, 1999), indicates a temperature increase during the PETM. In sum, palynofloral change at both northern and southern high paleolatitude sites suggests climate became warmer and wetter from the pre-PETM to PETM.

Middle latitude palynofloras also show distinct compositional change from the pre-PETM to the PETM. Seven sites record a rapid increase in Arecaceae (palm) and Bombacoideae (silk cotton tree and relatives) pollen (see Table S7). Living species in these groups are major constituents in seasonally dry subtropical and tropical forests (Carvalho-Sobrinho et al., 2014; Joyal, 1996; Linares-Palomino & Alvarez, 2005; Pennington et al., 2009), suggesting a shift to warmer, drier, or more seasonally dry climates during the PETM. The concurrent reduction at middle paleolatitudes of pollen with affinity to Cupressaceae (see Table S7), which require wet substrates (Averyanov et al., 2009; LePage, 2003), is also consistent with a shift to drier conditions. The concurrent increase in Arecaceae pollen and reduction in Cupressaceae pollen abundance in the 22/11-N and Harrell cores (Eldrett et al., 2014; Sluijs et al., 2014) likely contributes to the distinctiveness of the PETM body in our NMDS analysis (Figure 3).

In the southern mid-latitudes palynofloral change is also consistent with the spread of tropical and seasonally dry tropical forests, as indicated by the increased abundance of Arecaceae (palm) pollen, including *Nypa* (mangrove palm), at four sites and cores (Table S7; see Baker & Couvreur, 2013 for climatic preferences of palms). The concurrent decline at the three New Zealand sites (Crouch & Visscher, 2003; Handley et al., 2011; Raine et al., 2009), in the abundance of Podocarpaceae (podocarps) that prefer wet-temperate climates (Hill & Gibson, 1986; Macphail, 1999), also suggests a transition to more seasonally dry climates during the PETM. The distinctiveness of the PETM body in the NMDS analysis of the Kumara-2 core (Figure 3) likely results from the increase in *Nypa* pollen and concurrent decrease in Podocarpaceae pollen abundance.

Palynofloral records from both northern and southern middle paleolatitude sites suggest climates became warmer and more seasonally dry from the pre-PETM to PETM. Despite differences in the dominant pollen types and the number of PETM exclusive palynotaxa at each site, all sites record changing floral composition across the PETM. The plant groups involved in these floral changes suggest a latitudinally differentiated precipitation response to the PETM, with temperatures increasing everywhere, but precipitation increasing at high paleolatitudes and decreasing or becoming more seasonal at middle paleolatitudes.

More seasonal or episodic precipitation regimes in middle paleolatitudes are thought to have enhanced erosion (e.g., Baczynski et al., 2016; Lyons et al., 2019; Schmitz & Pujalte, 2003, 2007) and therefore potential reworking of pre-Cenozoic and Paleocene spores and pollen during the PETM. Pre-Cenozoic palynotaxa have been recognized in numerous middle paleolatitude PETM palynological samples, including from the Kallo Borehole in Belgium (Steurbaut et al., 2003), St. Pankraz in Austria (Hofmann et al., 2011), and the Tremp Basin of northern Spain (Manners, 2014). In the Bighorn Basin, USA, some plant groups (i.e., Cupressaceae and Juglandaceae) are present during the PETM in the palynoflora but not in the megaflora (Wing et al., 2005). This has also been suggested to result from erosion of the underlying pre-PETM sediments (Wing & Currano, 2013). Reworking would reduce the distinctiveness of PETM palynofloras and may account for some PETM palynofloras not appearing as compositionally distinct as they might be. This may explain why the middle paleolatitude Bighorn Basin samples from the CIE body and recovery are not compositionally distinct in the NMDS ordination (Figure 3). In spite of reworking, terrestrial pollen and spores consistently demonstrate floral change across the PETM at middle and high latitudes.

4.2. Paleoclimatic Inferences Derived Using the Köppen Climate Approach

At high paleolatitudes, the NLRs of most spore and pollen taxa from PETM sites are consistent with warm month means of 10°C–22°C and cold month means of 0°C–18°C, though some NLRs grow in regions with a warm month mean >10°C and cold month mean ≤0°C. The only site where the NLR reconstruction of PETM climate is cooler than that of the late Paleocene is the Natiak O-44 core in Arctic Canada. This anomalous shift probably results from a decrease in the proportion of palynotaxa that can be assigned a NLR (see Supplementary Table S4) rather than an accurate paleoclimatic reconstruction. During the PETM, high paleolatitude palynofloras also have

a higher proportion of NLRs growing in climates with a cold month mean >18°C, supporting the existence of a climate considerably warmer than what is modeled. Consistent with our palynofloral derived Köppen climate estimations, other lines of proxy evidence suggest elevated precipitation and terrestrial runoff during the PETM at high paleolatitudes. These include hydrogen isotope (δ^2H) value enrichment of leaf waxes (Pagani et al., 2006); low salinity dinoflagellate cyst occurrences (Sluijs et al., 2006); and more negative tooth apatite ($\delta^{18}O$) derived from North Sea sharks (Zacke et al., 2009). TEX86 and GDGT paleothermometry also predict that sea surface temperatures near the Arctic increased 5°C–8°C during the PETM (Peterse et al., 2012; Sluijs et al., 2006; Weijers et al., 2007), consistent with the palynofloral-derived inferences. The elevated abundance of polycyclic aromatic hydrocarbons (PAHs) in the Artic during the PETM as reported by Denis et al. (2017), seems counterintuitive, but is consistent with the development of peat swamps, which, despite being wet most of the time are susceptible to wildfires when the organic accumulation dries out (Korasidis et al., 2016; Perry et al., 2014). In East Antarctica, the increase in kaolinite in marine cores during the PETM has been attributed to increases in chemical weathering caused by higher temperature and/or rainfall (Robert & Kennett, 1994). At ODP Site 690, Maud Rise, $\delta^{18}O$ and Mg/Ca ratios of benthic and planktonic foraminifera also suggest a deep-water temperature increase of up to 8°C (Kennett & Stott, 1991; Thomas et al., 2002) while sea surface temperatures in the southwest Pacific are suggested, based on TEX86, to increase 6°C during the PETM (Sluijs et al., 2011). As such, the climate conditions inferred using our Köppen climate type approach are consistent with other proxy-based estimates of warm and wet high paleolatitudes globally during the PETM (summarized in Carmichael et al., 2017).

At middle paleolatitudes, the NLRs of most spore and pollen taxa from PETM sites are consistent with warm month means of 10°C–22°C and cold month means of 0°C–18°C. At high paleolatitudes the proportion of NLRs growing in climates with the cold month mean >18°C increases from the pre-PETM into the PETM, even though the broad Köppen climate types we reconstructed showed little change. In agreement with our palynofloral derived Köppen climate estimations, several lines of evidence suggest increasingly warmer and seasonally dry climates in the middle paleolatitude Bighorn Basin during the PETM. These include floral composition and leaf shape (Wing & Currano, 2013; Wing et al., 2005); paleosol weathering indices and nodule formation/composition (Adams et al., 2011; Kraus & Riggins, 2007; Kraus et al., 2013; Woody et al., 2014); accelerated organic matter decay rates as inferred from n-alkanes (Baczynski et al., 2017, 2019); decreased body size of perissodactyls (Secord et al., 2012; Smith et al., 2009); and changes in ichnofossil assemblages (Smith et al., 2008). The development of these features can be attributed to seasonally intense precipitation, high temperatures, or a combination of both (Wing et al., 2005). Organic proxies from the eastern margin of North America also indicates that the regional climate became much warmer (8°C; Zachos et al., 2006) and more seasonally extreme during the PETM (Lyons et al., 2019). In middle paleolatitudes of Europe, the PETM interval coincides with the deposition of the Claret Conglomerate (Schmitz & Pujalte, 2007; Schmitz et al., 2001), smectite clay (Egger et al., 2005) and nitrogen isotope ($\delta^{15}N$) fluctuations (Storme et al., 2012) also attributed to intermittent rainfall and seasonally dry periods. Palynofloral inferences derived using our Köppen approach are consistent with other proxy-based estimates showing warmer and seasonally drier middle paleolatitudes globally during the PETM.

At low paleolatitudes, the NLRs of most spore and pollen taxa from the Mar 2X PETM site are consistent with tropical conditions prevailing during the PETM, with air temperatures >18°C during the coldest month of the year. Other evidence for warmer climates at low paleolatitudes during the PETM includes palygorskite deposition across Africa (Bolle & Adatte, 2001; Carmichael et al., 2017; Robert & Chamley, 1991), and TEX86 proxies from Nigeria (Frieling et al., 2017). An increase in δ^2H values also suggests decreased rainfall during the PETM (Carmichael et al., 2017), which resulted in more arid climates in eastern Africa (Handley et al., 2008).

Although Köppen climate types estimated here are generally consistent with other proxy-based estimates for pre-PETM and PETM climates, we acknowledge that the NLR method we use may underestimate the amount of climate change that occurred. We intentionally excluded some palynomorphs from the analysis because their extant crown groups diversified greatly into cooler climate zones during the middle to late Cenozoic. A group such as grasses that is highly diverse in middle and high latitudes today would shift the mode of the NLR distributions toward cooler climates, yet would be misleading about PETM vegetation because the extant diversity evolved long after the PETM. We preferred removing such groups on grounds that it is better they provide no information about paleoclimate than misleading information, but this is at the cost of reducing the number of living taxa used in the analysis. A related problem is that some PETM sites had relatively few palynotaxa of known taxonomic affinity, so that the inferred paleoclimate was based on few NLR distributions (see Supplementary Table S4). The

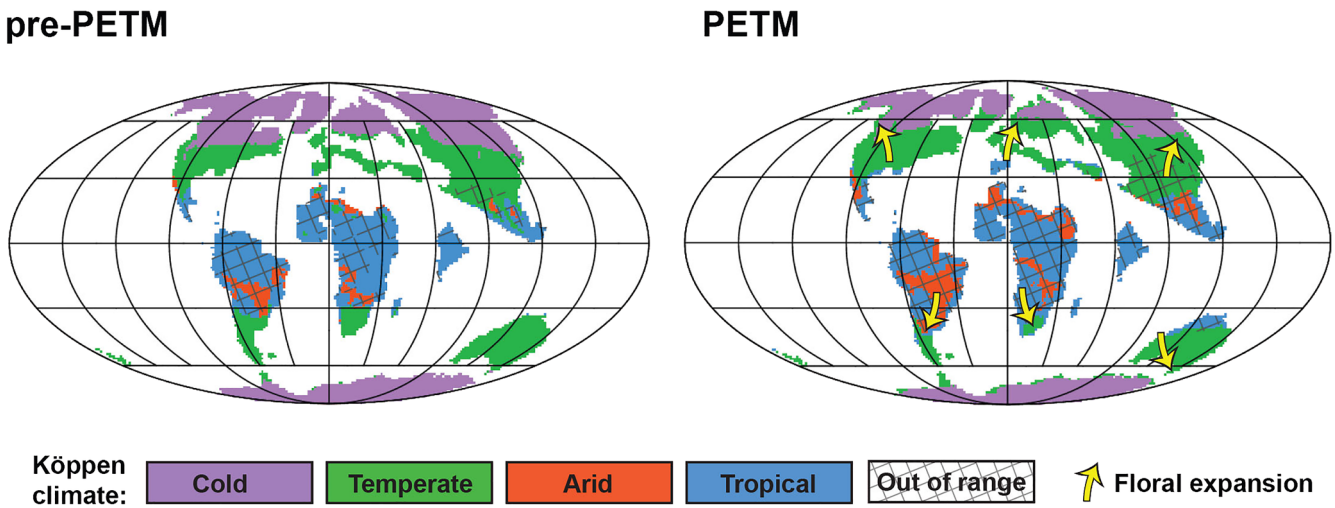

Figure 7. Changes in plant ranges from the pre-PETM to PETM mapped on simplified Köppen climate types. Palynofloral data (Table S7) and CESM simulations suggest that tropical and temperate (i.e., subtropical) climates expanded during the PETM, and that this occurred largely at the expense of cool climates. The CESM 1.2 simulation employs maximum orbital parameters.

relatively small shifts in Köppen climate types that we reconstruct at the PETM also reflects the relatively wide variation encompassed within each type. In spite of these problems it is likely that latitudinal climate gradients were shallower in the Paleocene-Eocene than they are today, and that the Köppen climate types inferred through NLR analyses successfully capture the major climatic features and changes for the pre-PETM and PETM.

4.3. Subtle Palynofloral Response to the PETM in the Tropics

In the low paleolatitudes palynofloral change from the pre-PETM to the PETM is not as great as it is at middle and high paleolatitudes. Low paleolatitude records of the Paleocene-Eocene do record subtle increases in the relative abundance of Arecaceae (palm), Bombacoideae (silk cotton tree and relatives) and Fabaceae (legume) pollen (see Table S7). These are groups with high present-day diversity in dry subtropical and tropical forest ecosystems (Joyal, 1996; Linares-Palomino & Alvarez, 2005; Pennington et al., 2009). In contrast to the modest changes in floral composition, the model predicts large increases in temperature and aridity, such that there is a great expansion in the area of the tropics occupied by climates with MAT >31.4°C, hotter than any modern climate (Figures 5 and 6). If we do not use the out of range climate type, the model predicts the expansion of tropical climate types with temperatures in the coldest month >18°C, arid climate types with mean annual temperatures >18°C and, for the Mar 2X site, a tropical desert (i.e., Aw; Figures 5 and 6). These hot desert conditions are modeled as being widespread at low paleolatitudes. The modeled shift from tropical wet to very hot and dry climate at Mar 2X is surprising given the modest changes in palynofloral composition at the site. The absence of major floral change at Mar 2X and other low paleolatitude palynofloral sites has several possible explanations. The PETM may not be well preserved, and especially in nearshore marine settings, reworking may have diluted or temporally smeared a distinctive PETM palynoflora. (Hiatuses can alternately create the false impression of rapid extinction, as happened in early analyses of the Harrell Core that did not recognize a gap at the base of the CIE (Harrington & Jaramillo, 2007; Sluijs et al., 2014)). It is also possible that the plant lineages present in pre-PETM time were able to tolerate climates outside the range of Earth's current climate, and thus the same taxa persisted. Finally, it may be that the modeled climates are hotter and more arid than what actually existed. Additional tropical data are needed to decide amongst these possible explanations.

4.4. Modeled and Proxy Climate Disparities

The model generated climates generally agree with proxy climate data on the expansion poleward of temperate and tropical climates at high and middle paleolatitudes during the PETM (Figure 7). At low paleolatitudes, the model predicts most regions are out of range (i.e., those with MATs exceeding 31.4°C), which prevents us from making explicit comparisons of NLR proxy estimates and models.

At high paleolatitudes, the model generated climate shows relatively warmer conditions during the PETM in comparison to the pre-PETM. This includes the expanded geographic distribution of temperate climate types at the expense of the cold climate types (Figure 7). For the high paleolatitude palynofloral sites investigated, the model predicts warm month means of 10°C–22°C and cold month means of 0°C–18°C for the temperate climate sites or ≤0°C for the cold climate site during the PETM. At high paleolatitudes there is good agreement between the model and proxy estimates during the PETM, which may result from the PETM model sufficiently warming the whole planet, so the predicted climates are closer to the proxy estimates. For the pre-PETM high paleolatitudes, it has proved difficult for the model to fully match the generally warm winter temperatures that proxy data imply (Contreras et al., 2014; Greenwood & West, 2017; Tripati et al., 2001; West et al., 2020). The equable climate enigma (Sloan, 1994; Sloan & Barron, 1990, 1992) has not been fully resolved.

At middle paleolatitudes, the model predicts increasingly warm conditions during the PETM in comparison to the pre-PETM, with the poleward expansion of tropical, arid and temperate climate types and the concurrent contraction of cold climate types (Figure 7). For the sites investigated, the model predicts warm month means of >10°C, the warmest month ≥22°C and cold month means of 0°C–18°C for the temperate climate sites and coldest month temperatures of >18°C for the tropical climate site. During the PETM there is generally good agreement between the model and proxy estimates, again perhaps because the PETM model sufficiently warms the Earth's surface, so the predicted climates are closer to the proxy estimates. For the pre-PETM continental interiors, the proxy reconstructions continue to be warmer and wetter than the model results for mid-latitude continental interiors, a long-standing problem (Currano et al., 2008; Fricke & Wing, 2004; Sloan, 1994; Sloan & Barron, 1990, 1992; Wing & Currano, 2013; Wing & Greenwood, 1993).

5. Conclusions

Data compiled from 38 sites where terrestrial spores and pollen have been reported from the Paleocene-Eocene transition reveal that PETM palynofloras generally have compositions distinct from pre-PETM samples at the same sites. These shifts in floral composition indicate changes in vegetation were global, although the taxa involved vary by region. NLR reconstructions of paleoclimate indicate that the PETM brought warmer and wetter climates to the high paleolatitudes in both hemispheres, but warmer and more seasonally dry climates to the middle paleolatitudes. The palynofloral climate reconstructions are consistent with other proxies indicating that precipitation shifted from middle to high paleolatitudes during the PETM (Carmichael et al., 2017, 2018; Hollis et al., 2019). Low paleolatitude sites are few, and paleoclimate reconstructions from NLR distributions are less certain because of the strong possibility that PETM climate at low latitudes was hotter, and possibly drier, than any extant low latitude climate. If so, the distributions of NLRs may not provide relevant information. In spite of this problem the lack of a compositionally distinct PETM palynoflora at Mar 2X is intriguing because it suggests the same lineages were able to persist in the area as climate warmed and dried substantially.

The Community Earth System Model (version CESM1.2) simulations generate climates that generally agree with NLR reconstructions, especially in the poleward expansion of temperate and tropical climates during the PETM. Model and proxy estimates are in greater agreement at high latitudes during the PETM than in the latest Paleocene, but for both periods the high northern paleolatitudes and continental interiors are colder in the model than in the NLR reconstructions. This suggests the long-standing equable climate enigma has not been fully resolved.

Acknowledgments
The authors thank all researchers whose data were incorporated in this work for their efforts to make their results accessible. P. Markwick is especially thanked for providing paleogeographic reconstructions. Lindsey Schwartz is also thanked for her assistance with the NMDS ordinations. We are grateful to Margot Cramwinckel and two anonymous reviewers for their constructive and helpful reviews on the manuscript. This work was supported by a Peter Buck Postdoctoral Fellowship to VAK.

Data Availability Statement

CESM1.2.2 is publicly available at http://www.cesm.ucar.edu/models/cesm1.2/ with modifications for deep time paleoclimate at https://github.com/CESM-Development/paleoToolkit/blob/master/cesm1_2/PaleoToolkit_Recipe_2020Jan1.pdf. Model output and GBIF floral occurrence data is publicly available at Korasidis et al. (2021).

References

Adams, J. S., Kraus, M. J., & Wing, S. L. (2011). Evaluating the use of weathering indices for determining mean annual precipitation in the ancient stratigraphic record. *Palaeogeography, Palaeoclimatology, Palaeoecology*, *309*(3–4), 358–366. https://doi.org/10.1016/j.palaeo.2011.07.004

Airy Shaw, H. K. (1974). Notes on Malesian and other Asiatic Euphorbiaceae. CLXXV. New species of *Austrobuxus* Miq., with a key to the whole genus. *Kew Bulletin*, *29*, 303–309.

Averyanov, L. V., Phan, K. L., Nguyen, T. H., Nguyen, S. K., Nguyen, T. V., & Pham, T. D. (2009). Preliminary observation of native *Glyptostrobus pensilis* (Taxodiaceae) stands in Vietnam. *Taiwania*, *54*(3), 191–212.

Baczynski, A. A., McInerney, F. A., Freeman, K. H., Wing, S. L., & Bighorn Basin Coring Project (BBCP) Science Team. (2019). Carbon isotope record of trace n-alkanes in a continental PETM section recovered by the Bighorn Basin Coring Project (BBCP). *Paleoceanography and Paleoclimatology*, *34*(5), 853–865. https://doi.org/10.1029/2019PA003579

Baczynski, A. A., McInerney, F. A., Wing, S. L., Kraus, M. J., Bloch, J. I., & Secord, R. (2017). Constraining paleohydrologic change during the Paleocene-Eocene Thermal Maximum in the continental interior of North America. *Palaeogeography, Palaeoclimatology, Palaeoecology*, *465*, 237–246. https://doi.org/10.1016/j.palaeo.2016.10.030

Baczynski, A. A., McInerney, F. A., Wing, S. L., Kraus, M. J., Morse, P. E., Bloch, J. I., et al. (2016). Distortion of carbon isotope excursion in bulk soil organic matter during the Paleocene-Eocene thermal maximum. *GSA Bulletin*, *128*(9–10), 1352–1366. https://doi.org/10.1130/B31389.1

Baker, W. J., & Couvreur, T. L. (2013). Global biogeography and diversification of palms sheds light on the evolution of tropical lineages. I. Historical biogeography. *Journal of Biogeography*, *40*(2), 274–285. https://doi.org/10.1111/j.1365-2699.2012.02795.x

Beck, H. E., Zimmermann, N. E., McVicar, T. R., Vergopolan, N., Berg, A., & Wood, E. F. (2018). Present and future Köppen-Geiger climate classification maps at 1-km resolution. *Scientific Data*, *5*(1), 1–12. https://doi.org/10.1038/sdata.2018.214

Berry, E. W. (1930). The past climate of the north polar region. *Smithsonian Miscellaneous Collections*, *82*(6), 1–29.

Bolle, M. P., & Adatte, T. (2001). Palaeocene-early Eocene climatic evolution in the Tethyan realm: Clay mineral evidence. *Clay Minerals*, *36*(2), 249–261.

Bouchal, J., Zetter, R., Grímsson, F., & Denk, T. (2014). Evolutionary trends and ecological differentiation in early Cenozoic Fagaceae of Western North America. *American Journal of Botany*, *101*(8), 1332–1349. https://doi.org/10.3732/ajb.1400118

Bowen, G. J., Bralower, T. J., Delaney, M. L., Dickens, G. R., Kelly, D. C., Koch, P. L., et al. (2006). Eocene hyperthermal event offers insight into greenhouse warming. *Eos, Transactions American Geophysical Union*, *87*(17), 165–169.

Carmichael, M. J., Inglis, G. N., Badger, M. P., Naafs, B. D. A., Behrooz, L., Remmelzwaal, S., et al. (2017). Hydrological and associated biogeochemical consequences of rapid global warming during the Paleocene-Eocene Thermal Maximum. *Global and Planetary Change*, *157*, 114–138. https://doi.org/10.1016/j.gloplacha.2017.07.014

Carmichael, M. J., Pancost, R. D., & Lunt, D. J. (2018). Changes in the occurrence of extreme precipitation events at the Paleocene-Eocene thermal maximum. *Earth and Planetary Science Letters*, *501*, 24–36. https://doi.org/10.1016/j.epsl.2018.08.005

Carvalho-Sobrinho, J. G., Alverson, W. S., Mota, A. C., Machado, M. C., & Baum, D. A. (2014). A new deciduous species of *Pachira* (Malvaceae: Bombacoideae) from a seasonally dry tropical forest in Northeastern Brazil. *Systematic Botany*, *39*(1), 260–267. https://doi.org/10.1600/036364414X678224

Contreras, L., Pross, J., Bijl, P. K., O'Hara, R. B., Raine, J. I., Sluijs, A., & Brinkhuis, H. (2014). Southern high-latitude terrestrial climate change during the Palaeocene-Eocene derived from a marine pollen record (ODP Site 1172, East Tasman Plateau). *Climate of the Past*, *10*(4), 1401–1420. https://doi.org/10.5194/cp-10-1401-2014

Crouch, E. M., & Visscher, H. (2003). Terrestrial vegetation record across the initial Eocene thermal maximum at the Tawanui marine section, New Zealand. *Geological Society of America Special Papers*, *369*, 351–363.

Currano, E. D., Wilf, P., Wing, S. L., Labandeira, C. C., Lovelock, E. C., & Royer, D. L. (2008). Sharply increased insect herbivory during the Paleocene-Eocene thermal maximum. *Proceedings of the National Academy of Sciences*, *105*(6), 1960–1964. https://doi.org/10.1073/pnas.0708646105

Denis, E. H., Pedentchouk, N., Schouten, S., Pagani, M., & Freeman, K. H. (2017). Fire and ecosystem change in the arctic across the Paleocene-Eocene thermal maximum. *Earth and Planetary Science Letters*, *467*, 149–156. https://doi.org/10.1016/j.epsl.2017.03.021

Denk, T., Grimm, G. W., Grímsson, F., & Zetter, R. (2013). Evidence from "Köppen signatures" of fossil plant assemblages for effective heat transport of Gulf Stream to subarctic North Atlantic during Miocene cooling. *Biogeosciences*, *10*(12), 7927–7942. https://doi.org/10.5194/bg-10-7927-2013

Dickens, G. R., Castillo, M. M., & Walker, J. C. (1997). A blast of gas in the latest Paleocene: Simulating first-order effects of massive dissociation of oceanic methane hydrate. *Geology*, *25*(3), 259–262. https://doi.org/10.1130/0091-7613(1997)025<0259:ABOGIT>2.3.CO

Dickens, G. R., O'Neil, J. R., Rea, D. K., & Owen, R. M. (1995). Dissociation of oceanic methane hydrate as a cause of the carbon isotope excursion at the end of the Paleocene. *Paleoceanography*, *10*(6), 965–971. https://doi.org/10.1029/95PA02087

Egger, H., Homayoun, M., Huber, H., Rögl, F., & Schmitz, B. (2005). Early Eocene climatic, volcanic, and biotic events in the northwestern Tethyan Untersberg section, Austria. *Palaeogeography, Palaeoclimatology, Palaeoecology*, *217*(3–4), 243–264. https://doi.org/10.1016/j.palaeo.2004.12.006

Eiserhardt, W. L., Svenning, J. C., Kissling, W. D., & Balslev, H. (2011). Geographical ecology of the palms (Arecaceae): Determinants of diversity and distributions across spatial scales. *Annals of Botany*, *108*(8), 1391–1416. https://doi.org/10.1093/aob/mcr146

Eldrett, J. S., Greenwood, D. R., Polling, M., Brinkhuis, H., & Sluijs, A. (2014). A seasonality trigger for carbon injection at the Paleocene-Eocene Thermal Maximum. *Climate of the Past*, *10*(2), 759–769. https://doi.org/10.5194/cp-10-759-2014

Fick, S. E., & Hijmans, R. J. (2017). WorldClim 2: New 1-km spatial resolution climate surfaces for global land areas. *International Journal of Climatology*, *37*(12), 4302–4315. https://doi.org/10.1002/joc.5086

Fletcher, T. L., Greenwood, D. R., Moss, P. T., & Salisbury, S. W. (2014). Paleoclimate of the late Cretaceous (Cenomanian-Turonian) portion of the Winton Formation, central-western Queensland, Australia: New observations based on CLAMP and bioclimatic analysis. *PALAIOS*, *29*(3), 121–128. https://doi.org/10.2110/palo.2013.080

Forster, P. I. (1997). A taxonomic revision of Austrobuxus Miq. (Euphorbiaceae: Dissiliariinae) in Australia. *Austrobaileya*, *4*, 619–626.

Frederiksen, N. O. (1980). Sporomorphs from the Jackson group (Upper Eocene) and adjacent strata of Mississippi and western Alabama (No. 1084, pp. 1–75). US Gov. Print. Off. https://doi.org/10.3133/pp1084

Fricke, H. C., & Wing, S. L. (2004). Oxygen isotope and paleobotanical estimates of temperature and δ18O-latitude gradients over North America during the early Eocene. *American Journal of Science*, *304*(7), 612–635. https://doi.org/10.2475/ajs.304.7.612

Frieling, J., Gebhardt, H., Huber, M., Adekeye, O. A., Akande, S. O., & Reichart, G. J. (2017). Extreme warmth and heat-stressed plankton in the tropics during the Paleocene-Eocene Thermal Maximum. *Science Advances*, *3*(3), e1600891. https://doi.org/10.1126/sciadv.1600891

Greenwood, D. R., & West, C. K. (2017). A fossil coryphoid palm from the Paleocene of Western Canada. *Review of Palaeobotany and Palynology*, *239*, 55–65. https://doi.org/10.1016/j.revpalbo.2016.12.002

Grimm, G. W., & Denk, T. (2012). Reliability and resolution of the coexistence approach—A revalidation using modern-day data. *Review of Palaeobotany and Palynology*, *172*, 33–47. https://doi.org/10.1016/j.revpalbo.2012.01.006

Grímsson, F., Zetter, R., Grimm, G. W., Pedersen, G. K., Pedersen, A. K., & Denk, T. (2015). Fagaceae pollen from the early Cenozoic of west Greenland: Revisiting Engler's and Chaney's Arcto-Tertiary hypotheses. *Plant Systematics and Evolution*, *301*(2), 809–832. https://doi.org/10.1007/s00606-014-1118-5

Guenther, A. B., Jiang, X., Heald, C. L., Sakulyanontvittaya, T., Duhl, T., Emmons, L. K., & Wang, X. (2012). The model of emissions of gases and aerosols from nature version 2.1 (MEGAN2.1): An extended and updated framework for modeling biogenic emissions. *Geoscience Model Development*, *5*, 1471–1492. https://doi.org/10.5194/gmd-5-1471-2012

Handley, L., Crouch, E. M., & Pancost, R. D. (2011). A New Zealand record of sea level rise and environmental change during the Paleocene-Eocene Thermal Maximum. *Palaeogeography, Palaeoclimatology, Palaeoecology*, *305*(1–4), 185–200. https://doi.org/10.1016/j.palaeo.2011.03.001

Handley, L., Pearson, P. N., McMillan, I. K., & Pancost, R. D. (2008). Large terrestrial and marine carbon and hydrogen isotope excursions in a new Paleocene/Eocene boundary section from Tanzania. *Earth and Planetary Science Letters*, *275*(1–2), 17–25. https://doi.org/10.1016/j.epsl.2008.07.030

Harbert, R. S., & Nixon, K. C. (2015). Climate reconstruction analysis using coexistence likelihood estimation (CRACLE): A method for the estimation of climate using vegetation. *American Journal of Botany*, *102*(8), 1277–1289. https://doi.org/10.3732/ajb.1400500

Harrington, G. J., & Jaramillo, C. A. (2007). Paratropical floral extinction in the late Palaeocene-early Eocene. *Journal of the Geological Society*, *164*(2), 323–332. https://doi.org/10.1144/0016-76492006-027

Heer, O. (1870). Die Miocene flora und fauna Spitzbergens. *Flora Fossilis Artica*, *1–3*, 1–98.

Herold, N., Buzan, J., Seton, M., Goldner, A., Green, J. A. M., Müller, R. D., et al. (2014). A suite of early Eocene (~55 Ma) climate model boundary conditions. *Geoscientific Model Development*, *7*(5), 2077–2090. https://doi.org/10.5194/gmd-7-2077-2014

Hill, R. S., & Gibson, N. (1986). Macrofossil evidence for the evolution of the alpine and subalpine vegetation of Tasmania. In A.Barlow (Ed.), *Flora and fauna of alpine Australasia: Ages and origins* (pp. 205–217). Melbourne: CSIRO.

Hofmann, C. C., Mohamed, O., & Egger, H. (2011). A new terrestrial palynoflora from the Palaeocene/Eocene boundary in the northwestern Tethyan realm (St. Pankraz, Austria). *Review of Palaeobotany and Palynology*, *166*(3–4), 295–310. https://doi.org/10.1016/j.revpalbo.2011.06.003

Hollis, C. J., Dunkley Jones, T., Anagnostou, E., Bijl, P. K., Cramwinckel, M. J., Cui, Y., et al. (2019). The DeepMIP contribution to PMIP4: Methodologies for selection, compilation and analysis of latest Paleocene and early Eocene climate proxy data, incorporating version 0.1 of the DeepMIP database. *Geoscientific Model Development*, *12*(7), 3149–3206. https://doi.org/10.5194/gmd-12-3149-2019

Huurdeman, E. P., Frieling, J., Reichgelt, T., Bijl, P. K., Bohaty, S. M., Holdgate, G. R., et al. (2021). Rapid expansion of meso-megathermal rain forests into the southern high latitudes at the onset of the Paleocene-Eocene Thermal Maximum. *Geology*, *49*(1), 40–44. https://doi.org/10.1130/G47343.1

Jagels, R., & Equiza, M. A. (2005). Competitive advantages of *Metasequoia* in warm high latitudes. In *The geobiology and ecology of Metasequoia* (pp. 335–349). Dordrecht: Springer.

Jones, T. D., Lunt, D. J., Schmidt, D. N., Ridgwell, A., Sluijs, A., Valdes, P. J., & Maslin, M. (2013). Climate model and proxy data constraints on ocean warming across the Paleocene-Eocene Thermal Maximum. *Earth-Science Reviews*, *125*, 123–145.

Joyal, E. (1996). The palm has its time: An ethnoecology of *Sabal uresana* in Sonora, Mexico. *Economic Botany*, *50*(4), 446–462. https://doi.org/10.1007/BF02866527

Kadereit, G., Borsch, T., Weising, K., & Freitag, H. (2003). Phylogeny of Amaranthaceae and Chenopodiaceae and the evolution of C4 photosynthesis. *International Journal of Plant Sciences*, *164*(6), 959–986. https://doi.org/10.1086/378649

Kennett, J. P., & Stott, L. D. (1991). Abrupt deep-sea warming, palaeoceanographic changes and benthic extinctions at the end of the Palaeocene. *Nature*, *353*(6341), 225–229. https://doi.org/10.1038/353225a0

Kiehl, J. T., Shields, C. A., Snyder, M. A., Zachos, J. C., & Rothstein, M. (2018). Greenhouse-and orbital-forced climate extremes during the early Eocene. *Philosophical Transactions of the Royal Society A: Mathematical, Physical & Engineering Sciences*, *376*(2130), 20170085. https://doi.org/10.1098/rsta.2017.0085

Kiehl, J. T., Zarzycki, C. M., Shields, C. A., & Rothstein, M. V. (2021). Simulated changes to tropical cyclones across the Paleocene-Eocene Thermal Maximum (PETM) boundary. *Palaeogeography, Palaeoclimatology, Palaeoecology*, *572*, 110421. https://doi.org/10.1016/j.palaeo.2021.110421

Köppen, W., & Geiger, R. (1936). *Das geographische System der Klimate* (pp. 1–44). Berlin, Germany: Gebrüder Borntraeger.

Korasidis, V. A., Shields, C. A., Wing, S. L., & Kiehl, J. T. (2021). Korasidis_etal_Paleooceanograhy_Paleoclimatology [Dataset]. Paleoceanograhy and Paleoclimatology. Zenodo. https://doi.org/10.5281/zenodo.5762604

Korasidis, V. A., Wallace, M. W., Wagstaff, B. E., Holdgate, G. R., Tosolini, A. M. P., & Jansen, B. (2016). Cyclic floral succession and fire in a Cenozoic wetland/peatland system. *Palaeogeography, Palaeoclimatology, Palaeoecology*, *461*, 237–252. https://doi.org/10.1016/j.palaeo.2016.08.030

Kottek, M., Grieser, J., Beck, C., Rudolf, B., & Rubel, F. (2006). World map of the Köppen-Geiger climate classification updated.

Kraus, M. J., McInerney, F. A., Wing, S. L., Secord, R., Baczynski, A. A., & Bloch, J. I. (2013). Paleohydrologic response to continental warming during the Paleocene-Eocene thermal maximum, Bighorn Basin, Wyoming. *Palaeogeography, Palaeoclimatology, Palaeoecology*, *370*, 196–208. https://doi.org/10.1016/j.palaeo.2012.12.008

Kraus, M. J., & Riggins, S. (2007). Transient drying during the Paleocene-Eocene thermal maximum (PETM): Analysis of paleosols in the Bighorn Basin, Wyoming. *Palaeogeography, Palaeoclimatology, Palaeoecology*, *245*(3–4), 444–461. https://doi.org/10.1016/j.palaeo.2006.09.011

Lawrence, D. M., Oleson, K. W., Flanner, M. G., Thornton, P. E., Swenson, S. C., Lawrence, P. J., et al. (2011). Parameterization improvements and functional and structural advances in version 4 of the community land model. *Journal of Advances in Modeling Earth Systems*, *3*, M03001. https://doi.org/10.1029/2011MS00045

LePage, B. A. (2003). A new species of *Thuja* (Cupressaceae) from the late Cretaceous of Alaska: Implications of being evergreen in a polar environment. *American Journal of Botany*, *90*(2), 167–174. https://doi.org/10.3732/ajb.90.2.167

Linares-Palomino, R., & Alvarez, S. I. P. (2005). Tree community patterns in seasonally dry tropical forests in the Cerros de Amotape Cordillera, Tumbes, Peru. *Forest Ecology and Management*, *209*(3), 261–272. https://doi.org/10.1016/j.foreco.2005.02.003

Lunt, D. J., Huber, M., Anagnostou, E., Baatsen, M. L. J., Caballero, R., DeConto, R., et al. (2017). The DeepMIP contribution to PMIP4: Experimental design for model simulations of the EECO, PETM, and pre-PETM (version 1.0). *Geoscientific Model Development*, *10*, 889–901. https://doi.org/10.5194/gmd-10-889-2017

Lyons, S. L., Baczynski, A. A., Babila, T. L., Bralower, T. J., Hajek, E. A., Kump, L. R., et al. (2019). Palaeocene-Eocene thermal maximum prolonged by fossil carbon oxidation. *Nature Geoscience*, *12*, 54–60. https://doi.org/10.1038/s41561-018-0277-3

Macphail, M. K. (1999). Palynostratigraphy of the Murray basin, inland southeastern Australia. *Palynology*, *23*(1), 197–240. https://doi.org/10.1080/01916122.1999.9989528

Manchester, S. R., & Dilcher, D. L. (1997). Reproductive and vegetative morphology of *Polyptera* (Juglandaceae) from the Paleocene of Wyoming and Montana. *American Journal of Botany*, *84*(5), 649–663. https://doi.org/10.2307/2445902

Manchester, S. R., Grímsson, F., & Zetter, R. (2015). Assessing the fossil record of asterids in the context of our current phylogenetic framework. *Annals of the Missouri Botanical Garden*, *100*(4), 329. https://doi.org/10.3417/2014033

Manchester, S. R., Pigg, K. B., & Crane, P. R. (2004). *Palaeocarpinus dakotensis* sp. n. (Betulaceae: Coryloideae) and associated staminate catkins, pollen, and leaves from the Paleocene of North Dakota. *International Journal of Plant Sciences*, *165*(6), 1135–1148. https://doi.org/10.1086/423870

Mandel, J. R., Dikow, R. B., Siniscalchi, C. M., Thapa, R., Watson, L. E., & Funk, V. A. (2019). A fully resolved backbone phylogeny reveals numerous dispersals and explosive diversifications throughout the history of Asteraceae. *Proceedings of the National Academy of Sciences*, *116*(28), 14083–14088. https://doi.org/10.1073/pnas.1903871116

Manners, H. R. (2014). *A multi-proxy study of the Palaeocene-Eocene Thermal Maximum in northern Spain* (Doctoral dissertation). University of Plymouth. Retrieved from PEARL http://hdl.handle.net/10026.1/2895

McInerney, F. A., & Wing, S. L. (2011). The Paleocene-Eocene thermal maximum: A perturbation of carbon cycle, climate, and biosphere with implications for the future. *Annual Review of Earth and Planetary Sciences*, *39*, 489–516. https://doi.org/10.1146/annurev-earth-040610-133431

McIver, E. E., & Basinger, J. F. (1999). Early Tertiary floral evolution in the Canadian high Arctic. *Annals of the Missouri Botanical Garden*, *86*(2), 523–545. https://doi.org/10.2307/2666184

McNeil, D. H., Parsons, M. G., & Russel-Houston, J. (2013). The Paleocene-Eocene thermal maximum in the Arctic Beaufort-Mackenzie Basin—Palynomorphs, carbon isotopes and benthic foraminiferal turnover. *Bulletin of Canadian Petroleum Geology*, *61*(2), 157–186. https://doi.org/10.2113/gscpgbull.61.2.157

Mitchell, T. C., Williams, B. R., Wood, J. R., Harris, D. J., Scotland, R. W., & Carine, M. A. (2016). How the temperate world was colonised by bindweeds: Biogeography of the Convolvuleae (Convolvulaceae). *BMC Evolutionary Biology*, *16*(1), 1–12. https://doi.org/10.1186/s12862-016-0591-6

Neale, R. B., Chen, C. C., Gettelman, A., Lauritzen, P. H., Park, S., Williamson, D. L., et al. (2010). *Description of the NCAR community atmosphere model (CAM5.0)*. NCAR Tech. Rep. NCAR/TN-486 + STR (268 pp.).

Pagani, M., Pedentchouk, N., Huber, M., Sluijs, A., Schouten, S., Brinkhuis, H., et al. (2006). Arctic hydrology during global warming at the Palaeocene/Eocene thermal maximum. *Nature*, *442*(7103), 671–675. https://doi.org/10.1038/nature05043

Park, S., Bretherton, C. S., & Rasch, P. J. (2014). Integrating cloud processes in the community atmosphere model, Version 5. *Journal of Climate*, *27*, 6821–6856. https://doi.org/10.1175/JCLI-D-14-00087.1

Partridge, A. D. (2004). The ancient conifers and great lakes of Bass Strait. *Field Nats News*, *134*, 1–3.

Pennington, R. T., Lavin, M., & Oliveira-Filho, A. (2009). Woody plant diversity, evolution, and ecology in the tropics: Perspectives from seasonally dry tropical forests. *Annual Review of Ecology, Evolution, and Systematics*, *40*, 437–457. https://doi.org/10.1146/annurev.ecolsys.110308.120327

Peppe, D. J., Baumgartner, A., Flynn, A., & Blonder, B. (2018). Reconstructing paleoclimate and paleoecology using fossil leaves. In *Methods in paleoecology* (pp. 289–317). Cham: Springer.

Perry, G. L., Wilmshurst, J. M., & McGlone, M. S. (2014). Ecology and long-term history of fire in New Zealand. *New Zealand Journal of Ecology*, 157–176. Retrieved from http://www.jstor.org/stable/24060795

Peterse, F., van der Meer, J., Schouten, S., Weijers, J. W., Fierer, N., Jackson, R. B., et al. (2012). Revised calibration of the MBT-CBT paleotemperature proxy based on branched tetraether membrane lipids in surface soils. *Geochimica et Cosmochimica Acta*, *96*, 215–229. https://doi.org/10.1016/j.gca.2012.08.011

Pocknall, D. T. (1987). Palynomorph biozones for the fort Union and Wasatch formations (upper Paleocene-lower Eocene), powder river basin, Wyoming and Montana, USA. *Palynology*, *11*(1), 23–35. https://doi.org/10.1080/01916122.1987.9989316

Punyasena, S. W. (2008). Estimating Neotropical palaeotemperature and palaeoprecipitation using plant family climatic optima. *Palaeogeography, Palaeoclimatology, Palaeoecology*, *265*(3–4), 226–237. https://doi.org/10.1016/j.palaeo.2008.04.025

Raine, J. I., Kennedy, E. M., & Crouch, E. M. (2009). New Zealand Paleogene vegetation and climate. *Climatic and Biotic events of the Paleogene, GNS Science Miscellaneous Series*, *18*, 117–122.

Reichgelt, T., West, C. K., & Greenwood, D. R. (2018). The relation between global palm distribution and climate. *Scientific Reports*, *8*(1), 1–11. https://doi.org/10.1038/s41598-018-23147-2

Richter, S. L., & LePage, B. A. (2005). A high-resolution palynological analysis, Axel Heiberg Island, Canadian High Arctic. In B. A. LePage, C. J. Williams, & H. Yang (Eds.), *The geobiology and ecology of Metasequoia* (pp. 137–158). Dordrecht: Springer.

Robert, C., & Chamley, H. (1991). Development of early Eocene warm climates, as inferred from clay mineral variations in oceanic sediments. *Palaeogeography, Palaeoclimatology, Palaeoecology*, *89*(4), 315–331.

Robert, C., & Kennett, J. P. (1994). Antarctic subtropical humid episode at the Paleocene-Eocene boundary: Clay-mineral evidence. *Geology*, *22*(3), 211–214. https://doi.org/10.1130/0091-7613(1994)022<0211:ASHEAT>2.3.CO;2

Rush, W. D., Kiehl, J. T., Shields, C. A., & Zachos, J. C. (2021). Increased frequency of extreme precipitation events in the North Atlantic during the PETM: Observations and theory. *Palaeogeography, Palaeoclimatology, Palaeoecology*, 110289. https://doi.org/10.1016/j.palaeo.2021.110289

Schmitz, B., & Pujalte, V. (2003). Sea-level, humidity, and land-erosion records across the initial Eocene thermal maximum from a continental-marine transect in northern Spain. *Geology*, *31*(8), 689–692. https://doi.org/10.1130/G19527.1

Schmitz, B., & Pujalte, V. (2007). Abrupt increase in seasonal extreme precipitation at the Paleocene-Eocene boundary. *Geology*, *35*(3), 215–218. https://doi.org/10.1130/G23261A.1

Schmitz, B., Pujalte, V., & Nunez-Betelu, K. (2001). Climate and sea-level perturbations during the Incipient Eocene thermal maximum: Evidence from siliciclastic units in the Basque basin (Ermua, Zumaia and Trabakua Pass), northern Spain. *Palaeogeography, Palaeoclimatology, Palaeoecology*, *165*(3–4), 299–320. https://doi.org/10.1016/S0031-0182(00)00167-X

Secord, R., Bloch, J. I., Chester, S. G., Boyer, D. M., Wood, A. R., Wing, S. L., et al. (2012). Evolution of the earliest horses driven by climate change in the Paleocene-Eocene Thermal Maximum. *Science*, *335*(6071), 959–962. https://doi.org/10.1126/science.1213859

Shields, C. A., Kiehl, J. T., Rush, W., Rothstein, M., & Snyder, M. A. (2021). Atmospheric rivers in high-resolution simulations of the Paleocene Eocene thermal maximum (PETM). *Palaeogeography, Palaeoclimatology, Palaeoecology*, 110293. https://doi.org/10.1016/j.palaeo.2021.110293

Sloan, L. C. (1994). Equable climates during the early Eocene: Significance of regional paleogeography for North American climate. *Geology*, *22*(10), 881–884. https://doi.org/10.1130/0091-7613(1994)022<0881:ECDTEE>2.3.CO;2

Sloan, L. C., & Barron, E. J. (1990). "Equable" climates during Earth history? *Geology*, *18*(6), 489–492. https://doi.org/10.1130/0091-7613(1990)018<0489:ECDEH>2.3.CO;2

Sloan, L. C., & Barron, E. J. (1992). A comparison of Eocene climate model results to quantified paleoclimatic interpretations. *Palaeogeography, Palaeoclimatology, Palaeoecology*, *93*(3–4), 183–202. https://doi.org/10.1016/0031-0182(92)90096-N

Sluijs, A., Bijl, P. K., Schouten, S., Röhl, U., Reichart, G. J., & Brinkhuis, H. (2011). Southern ocean warming, sea level and hydrological change during the Paleocene-Eocene thermal maximum. *Climate of the Past*, *7*(1), 47–61. https://doi.org/10.5194/cp-7-47-2011

Sluijs, A., Schouten, S., Pagani, M., Woltering, M., Brinkhuis, H., Damsté, J. S. S., et al. (2006). Subtropical arctic ocean temperatures during the Palaeocene/Eocene thermal maximum. *Nature*, *441*(7093), 610–613. https://doi.org/10.1038/nature04668

Sluijs, A., Van Roij, L., Harrington, G. J., Schouten, S., Sessa, J. A., LeVay, L. J., et al. (2014). Warming, euxinia and sea level rise during the Paleocene-Eocene thermal maximum on the Gulf Coastal Plain: Implications for ocean oxygenation and nutrient cycling. *Climate of the Past*, *10*(4), 1421–1439. https://doi.org/10.5194/cp-10-1421-2014

Smith, J. J., Hasiotis, S. T., Kraus, M. J., & Woody, D. T. (2008). Relationship of floodplain ichnocoenoses to paleopedology, paleohydrology, and paleoclimate in the Willwood formation, Wyoming, during the Paleocene-Eocene thermal maximum. *PALAIOS*, *23*(10), 683–699. https://doi.org/10.2110/palo.2007.p07-080r

Smith, J. J., Hasiotis, S. T., Kraus, M. J., & Woody, D. T. (2009). Transient dwarfism of soil fauna during the Paleocene-Eocene thermal maximum. *Proceedings of the National Academy of Sciences*, *106*(42), 17655–17660. https://doi.org/10.1073/pnas.0909674106

Soreng, R. J., Peterson, P. M., Romaschenko, K., Davidse, G., Zuloaga, F. O., Judziewicz, E. J., et al. (2015). A worldwide phylogenetic classification of the Poaceae (Gramineae). *Journal of Systematics and Evolution*, *53*(2), 117–137. https://doi.org/10.1111/jse.12150

Steurbaut, E., Magioncalda, R., Dupuis, C., Van Simaeys, S., Roche, E., & Roche, M. (2003). Palynology, paleoenvironments, and organic carbon isotope evolution in lagoonal Paleocene-Eocene boundary settings in North Belgium. *Geological Society of America Special Papers*, *369*, 291–317.

Storme, J. Y., Dupuis, C., Schnyder, J., Quesnel, F., Garel, S., Iakovleva, A. I., et al. (2012). Cycles of humid-dry climate conditions around the P/E boundary: New stable isotope data from terrestrial organic matter in Vasterival section (NW France). *Terra Nova*, *24*(2), 114–122. https://doi.org/10.1111/j.1365-3121.2011.01044.x

Suan, G., Popescu, S. M., Suc, J. P., Schnyder, J., Fauquette, S., Baudin, F., et al. (2017). Subtropical climate conditions and mangrove growth in Arctic Siberia during the early Eocene. *Geology*, *45*(6), 539–542. https://doi.org/10.1130/G38547.1

Suc, J. P., Fauquette, S., Popescu, S. M., & Robin, C. (2020). Subtropical mangrove and evergreen forest reveal Paleogene terrestrial climate and physiography at the North Pole. *Palaeogeography, Palaeoclimatology, Palaeoecology*, *551*, 109755. https://doi.org/10.1016/j.palaeo.2020.109755

Svenning, J. C., Borchsenius, F., Bjorholm, S., & Balslev, H. (2008). High tropical net diversification drives the New World latitudinal gradient in palm (Arecaceae) species richness. *Journal of Biogeography*, *35*(3), 394–406. https://doi.org/10.1111/j.1365-2699.2007.01841.x

Theerawitaya, C., Samphumphaung, T., Cha-um, S., Yamada, N., & Takabe, T. (2014). Responses of Nipa palm (*Nypa fruticans*) seedlings, a mangrove species, to salt stress in pot culture. *Flora-Morphology, Distribution, Functional Ecology of Plants*, *209*(10), 597–603. https://doi.org/10.1016/j.flora.2014.08.004

Thomas, D. J., Zachos, J. C., Bralower, T. J., Thomas, E., & Bohaty, S. (2002). Warming the fuel for the fire: Evidence for the thermal dissociation of methane hydrate during the Paleocene-Eocene thermal maximum. *Geology*, *30*(12), 1067–1070. https://doi.org/10.1130/0091-7613(2002)030<1067:WTFFTF>2.0.CO;2

Thornhill, A. H., Popple, L. W., Carter, R. J., Ho, S. Y., & Crisp, M. D. (2012). Are pollen fossils useful for calibrating relaxed molecular clock dating of phylogenies? A comparative study using Myrtaceae. *Molecular Phylogenetics and Evolution*, *63*(1), 15–27. https://doi.org/10.1016/j.ympev.2011.12.003

Tiffney, B. H. (1994). An estimate of the early Tertiary paleoclimate of the southern arctic. In M. C.Boulter, & H. C.Fisher (Eds.), *Cenozoic plants and climates of the Arctic. NATO ASI Series. Series I: Global environmental change* (Vol. 27). Berlin, Heidelberg: Springer. https://doi.org/10.1007/978-3-642-79378-3_19

Tripati, A., Zachos, J., Marincovich, L., Jr., & Bice, K. (2001). Late Paleocene Arctic coastal climate inferred from molluscan stable and radiogenic isotope ratios. *Palaeogeography, Palaeoclimatology, Palaeoecology*, *170*(1–2), 101–113. https://doi.org/10.1016/S0031-0182(01)00230-9

Tryon, R. M., & Tryon, A. F. (2012). *Ferns and allied plants: With special reference to tropical America*. Springer Science & Business Media.

Tschudy, R. (1969). Relationship of palynomorphs to sedimentation. In R. Tschudy, & R. Scott (Eds.), *Aspects of palynology* (pp. 79–96). New York: John Wiley and Sons.

Utescher, T., Bruch, A. A., Erdei, B., François, L., Ivanov, D., Jacques, F. M. B., et al. (2014). The Coexistence Approach—Theoretical background and practical considerations of using plant fossils for climate quantification. *Palaeogeography, Palaeoclimatology, Palaeoecology*, *410*, 58–73. https://doi.org/10.1016/j.palaeo.2014.05.031

Vajda, V., & McLoughlin, S. (2005). Upptackten av ett Levande Fossil-*Wollemia* (Discovery of a living fossil-Wollemi pine). *Svensk Botanisk Tidskrift*, *99*(6), 295–302.

Webster, G. L. (1994). Classification of the Euphorbiaceae. *Annals of the Missouri Botanical Garden*, *81*, 3–32. https://doi.org/10.2307/2399908

Weijers, J. W., Schouten, S., Sluijs, A., Brinkhuis, H., & Damsté, J. S. S. (2007). Warm arctic continents during the Palaeocene-Eocene thermal maximum. *Earth and Planetary Science Letters*, *261*(1–2), 230–238. https://doi.org/10.1016/j.epsl.2007.06.033

West, C. K., Greenwood, D. R., Reichgelt, T., Lowe, A. J., Vachon, J. M., & Basinger, J. F. (2020). Paleobotanical proxies for early Eocene climates and ecosystems in northern North America from middle to high latitudes. *Climate of the Past*, *16*(4), 1387–1410. https://doi.org/10.5194/cp-16-1387-2020

Westerhold, T., Röhl, U., Donner, B., & Zachos, J. C. (2018). Global extent of early Eocene hyperthermal events: A new Pacific benthic foraminiferal isotope record from Shatsky rise (ODP site 1209). *Paleoceanography and Paleoclimatology*, *33*(6), 626–642. https://doi.org/10.1029/2017PA003306

Willard, D. A., Donders, T. H., Reichgelt, T., Greenwood, D. R., Sangiorgi, F., Peterse, F., et al. (2019). Arctic vegetation, temperature, and hydrology during Early Eocene transient global warming events. *Global and Planetary Change*, *178*, 139–152. https://doi.org/10.1016/j.gloplacha.2019.04.012

Wing, S. L., & Currano, E. D. (2013). Plant response to a global greenhouse event 56 million years ago. *American Journal of Botany*, *100*(7), 1234–1254. https://doi.org/10.3732/ajb.1200554

Wing, S. L., & Greenwood, D. R. (1993). Fossils and fossil climate: The case for equable continental interiors in the Eocene. *Philosophical Transactions of the Royal Society of London. Series B: Biological Sciences*, *341*(1297), 243–252. https://doi.org/10.1098/rstb.1993.0109

Wing, S. L., Harrington, G. J., Smith, F. A., Bloch, J. I., Boyer, D. M., & Freeman, K. H. (2005). Transient floral change and rapid global warming at the Paleocene-Eocene boundary. *Science*, *310*(5750), 993–996. https://doi.org/10.1126/science.1116913

Wolfe, J. A. (1971). Tertiary climatic fluctuations and methods of analysis of Tertiary floras. *Palaeogeography, Palaeoclimatology, Palaeoecology*, *9*(1), 27–57. https://doi.org/10.1016/0031-0182(71)90016-2

Woody, D. T., Smith, J. J., Kraus, M. J., & Hasiotis, S. T. (2014). Manganese-bearing rhizocretions in the Willwood formation, Wyoming, USA: Implications for paleoclimate during the Paleocene-Eocene thermal maximum. *PALAIOS*, *29*(6), 266–276. https://doi.org/10.2110/palo.2013.105

Zachos, J. C., Schouten, S., Bohaty, S., Quattlebaum, T., Sluijs, A., Brinkhuis, H., et al. (2006). Extreme warming of mid-latitude coastal ocean during the Paleocene-Eocene Thermal Maximum: Inferences from TEX86 and isotope data. *Geology*, *34*(9), 737–740. https://doi.org/10.1130/G22522.1

Zacke, A., Voigt, S., Joachimski, M. M., Gale, A. S., Ward, D. J., & Tütken, T. (2009). Surface-water freshening and high-latitude river discharge in the Eocene North Sea. *Journal of the Geological Society*, *166*(5), 969–980. https://doi.org/10.1144/0016-76492008-068

Zeebe, R. E., & Lourens, L. J. (2019). Solar System chaos and the Paleocene-Eocene boundary age constrained by geology and astronomy. *Science*, *365*(6456), 926–929. https://doi.org/10.1126/science.aax0612

References From the Supporting Information

Adeonipekun, P. A., & Oyelami, A. (2015). Palynology of Late Paleocene-Earliest Eocene Outcrop Sediments from Benin Basin, SW Nigeria: Implications for Paleoclimatology and PETM Record in the Tropics. *Global Journal of Science Frontier Research: C Biological Science*, *15*(3), 2249–4626.

Aleksandrova, G. N., & Shcherbinina, E. A. (2011). Stratigraphy and paleoenvironmental interpretation of the Paleocene-Eocene transition in the Eastern Crimea. *Stratigraphy and Geological Correlation*, *19*(4), 424–449. https://doi.org/10.1134/S0869593811040022

Balme, B. E. (1995). Fossil in situ spores and pollen grains: An annotated catalogue. *Review of Palaeobotany and Palynology*, *87*(2-4), 81–323. https://doi.org/10.1016/0034-6667(95)93235-X

Barker, N. P., Weston, P. H., Rutschmann, F., & Sauquet, H. (2007). Molecular dating of the 'Gondwanan' plant family Proteaceae is only partially congruent with the timing of the break-up of Gondwana. *Journal of Biogeography*, *34*(12), 2012–2027. https://doi.org/10.1111/j.1365-2699.2007.01749.x

Bolkhovitina, N. A. (1961). Fossil and recent spores in the Schizaeaceae. *Trudy*.

Carpenter, R. J., & Milne, L. A. (2020). New species of xeromorphic *Banksia* (Proteaceae) foliage and *Banksia*-like pollen from the late Eocene of Western Australia. *Australian Journal of Botany*, *68*(3), 165–178. https://doi.org/10.1071/BT19110

Cieraad, E., & Lee, D. E. (2006). The New Zealand fossil record of ferns for the past 85 million years. *New Zealand Journal of Botany*, *44*(2), 143–170. https://doi.org/10.1080/0028825X.2006.9513015

Collinson, M. E., Steart, D. C., Harrington, G. J., Hooker, J. J., Scott, A. C., Allen, L. O., et al. (2009). Palynological evidence of vegetation dynamics in response to palaeoenvironmental change across the onset of the Paleocene-Eocene Thermal Maximum at Cobham, Southern England. *Grana*, *48*(1), 38–66. https://doi.org/10.1080/00173130802707980

Contreras, L., Pross, J., Bijl, P. K., O'Hara, R. B., Raine, J. I., Sluijs, A., et al. (2014). Southern high-latitude terrestrial climate change during the Palaeocene-Eocene derived from a marine pollen record (ODP Site 1172, East Tasman Plateau). *Climate of the Past*, *10*(4), 1401–1420. https://doi.org/10.5194/cp-10-1401-2014

Couper, R. A. (1960). New Zealand Mesozoic and Cainozoic plant microfossils. *New Zealand Geological Survey Paleontological Bulletin*, *32*, 1–87.

Crouch, E. M., & Visscher, H. (2003). Terrestrial vegetation record across the initial Eocene thermal maximum at the Tawanui marine section, New Zealand. *Geological Society of America Special Papers*, *369*, 351–363.

Daly, R. J., Jolley, D. W., & Spicer, R. A. (2011). The role of angiosperms in Palaeocene Arctic ecosystems: A palynological study from the Alaskan North Slope. *Palaeogeography, Palaeoclimatology, Palaeoecology*, *309*(3-4), 374–382. https://doi.org/10.1016/j.palaeo.2011.07.007

Demchuk, T., Denison, C., Gardner, K., Stephenson, M., & O'Keefe, J. (2019). Multidisciplinary characterization of the PETM hyperthermal event in Central Texas: Palynology, isotope chemistry and sedimentology. Presented at the 2019 AAPG Annual Convention and Exhibition.

Dettmann, M. (1994). Cretaceous vegetation: The microfossil record. In R.Hill (Ed.), *History of the Australian vegetation: Cretaceous to recent* (pp. 143–170). Cambridge University Press.

Dunn, R. (2019). Canopy dynamics and palynofloristic change during the PETM, Hanna Basin, Wyoming. Presented at the Terrestrial and Coastal Climates of the Paleocene-Eocene Thermal Maximum Workshop Abstracts.

El-Noamani, Z. M. (2018). Reconstruction of paleovegetation and paleoecology from the Early Cretaceous sporomorphs of Bougaz-1 well, northeast Sinai, Egypt. *Egyptian Journal of Botany*, *58*(3), 397–409. https://doi.org/10.21608/ejbo.2018.2810.1150

Frederiksen, N. O. (1979). Paleogene sporomorph biostratigraphy, northeastern Virginia. *Palynology*, *3*(1), 129–167.

Frederiksen, N. O. (1983). *Middle Eocene palynomorphs from San Diego, California (No. 12)*. American Association of Stratigraphic Palynologists Foundation.

Frederiksen, N. O. (1998). Upper Paleocene and lowermost Eocene angiosperm pollen biostratigraphy of the eastern Gulf Coast and Virginia. *Micropaleontology*, *44*(1), 45–68.

Frederiksen, N. O., & Christopher, R. A. (1978). Taxonomy and biostratigraphy of Late Cretaceous and Paleogene triatriate pollen from South Carolina. *Palynology*, *2*(1), 113–145.

Frieling, J., Huurdeman, E. P., Rem, C., Donders, T. H., Pross, J., Bohaty, S. M., et al. (2018). Identification of the Paleocene-Eocene boundary in coastal strata in the Otway Basin, Victoria, Australia. *Journal of Micropalaeontology*, *37*(1), 317–339. https://doi.org/10.5194/jm-37-317-2018

Garel, S., Schnyder, J., Jacob, J., Dupuis, C., Boussafir, M., Le Milbeau, C., et al. (2013). Paleohydrological and paleoenvironmental changes recorded in terrestrial sediments of the Paleocene-Eocene boundary (Normandy, France). *Palaeogeography, Palaeoclimatology, Palaeoecology*, *376*, 184–199. https://doi.org/10.1016/j.palaeo.2013.02.035

Gernandt, D. S., Magallón, S., Geada López, G., Zerón Flores, O., Willyard, A., & Liston, A. (2008). Use of simultaneous analyses to guide fossil-based calibrations of Pinaceae phylogeny. *International Journal of Plant Sciences*, *169*(8), 1086–1099. https://doi.org/10.1086/590472

Handley, L., Crouch, E. M., & Pancost, R. D. (2011). A New Zealand record of sea level rise and environmental change during the Paleocene-Eocene Thermal Maximum. *Palaeogeography, Palaeoclimatology, Palaeoecology*, *305*(1-4), 185–200. https://doi.org/10.1016/j.palaeo.2011.03.001

Handley, L., O'Halloran, A., Pearson, P. N., Hawkins, E., Nicholas, C. J., Schouten, S., et al. (2012). Changes in the hydrological cycle in tropical East Africa during the Paleocene-Eocene Thermal Maximum. *Palaeogeography, Palaeoclimatology, Palaeoecology*, *329*, 10–21. https://doi.org/10.1016/j.palaeo.2012.02.002

Harbaugh, D. T., Nepokroeff, M., Rabeler, R. K., McNeill, J., Zimmer, E. A., & Wagner, W. L. (2010). A new lineage-based tribal classification of the family Caryophyllaceae. *International Journal of Plant Sciences*, *171*(2), 185–198. https://doi.org/10.1086/648993

Harding, I. C., Charles, A. J., Marshall, J. E., Pälike, H., Roberts, A. P., Wilson, P. A., et al. (2011). Sea-level and salinity fluctuations during the Paleocene-Eocene thermal maximum in Arctic Spitsbergen. *Earth and Planetary Science Letters*, *303*(1-2), 97–107. https://doi.org/10.1016/j.epsl.2010.12.043

Harrington, G. J. (1999). *North American palynofloral dynamics in the late Paleocene to early Eocene* (Doctoral dissertation). University of Sheffeild.

Harrington, G. J. (2008). Comparisons between Palaeocene-Eocene paratropical swamp and marginal marine pollen floras from Alabama and Mississippi, USA. *Palaeontology*, *51*(3), 611–622. https://doi.org/10.1111/j.1475-4983.2008.00768.x

Harrington, G. J., Clechenko, E. R., & Kelly, D. C. (2005). Palynology and organic-carbon isotope ratios across a terrestrial Palaeocene/Eocene boundary section in the Williston Basin, North Dakota, USA. *Palaeogeography, Palaeoclimatology, Palaeoecology*, *226*(3–4), 214–232. https://doi.org/10.1016/j.palaeo.2005.05.013

Harrington, G. J., & Kemp, S. J. (2001). US Gulf Coast vegetation dynamics during the latest Palaeocene. *Palaeogeography, Palaeoclimatology, Palaeoecology*, *167*(1–2), 1–21. https://doi.org/10.1016/S0031-0182(00)00228-5

Hofmann, C. C., Mohamed, O., & Egger, H. (2011). A new terrestrial palynoflora from the Palaeocene/Eocene boundary in the northwestern Tethyan realm (St. Pankraz, Austria). *Review of Palaeobotany and Palynology*, *166*(3-4), 295–310. https://doi.org/10.1016/j.revpalbo.2011.06.003

Homes, A. M., Cieraad, E., Lee, D. E., Lindqvist, J. K., Raine, J. I., Kennedy, E. M., et al. (2015). A diverse fern flora including macrofossils with *in situ* spores from the late Eocene of southern New Zealand. *Review of Palaeobotany and Palynology*, *220*, 16–28. https://doi.org/10.1016/j.revpalbo.2015.04.007

Huurdeman, E. P., Frieling, J., Reichgelt, T., Bijl, P. K., Bohaty, S. M., Holdgate, G. R., et al. (2021). Rapid expansion of meso-megathermal rain forests into the southern high latitudes at the onset of the Paleocene-Eocene Thermal Maximum. *Geology*, *49*(1), 40–44. https://doi.org/10.1130/G47343.1

Jaramillo, C., Hoorn, C., Silva, S. A., Leite, F., Herrera, F., Quiroz, L., et al. (2010). The origin of the modern Amazon rainforest: Implications of the palynological and palaeobotanical record. *Amazonia, Landscape and Species Evolution*, *317*, 334.

Jaramillo, C., Ochoa, D., Contreras, L., Pagani, M., Carvajal-Ortiz, H., Pratt, L. M., et al. (2010). Effects of rapid global warming at the Paleocene-Eocene boundary on neotropical vegetation. *Science*, *330*(6006), 957–961. https://doi.org/10.1126/science.1193833

Jaramillo, C. A., Moreno, E., Ramírez, V., da Silva-Caminha, S. A., da la Barrera, A., da la Barrera, A., et al. (2014). Palynological record of the last 20 Million years in Panama. In W. D.Stevens, O. M.Montiel, & P.Raven (Eds.), *Paleobotany and biogeography: A Festschrift for Alan Graham in his 80th year* (pp. 124–253). St. Louis: Missouri Botanical Garden Press.

Jardine, P. E. (2011). *Spatial and temporal diversity trends in an extra-tropical megathermal vegetation type: the early Palaeogene pollen and pore record from the US Gulf Coast* (Doctoral dissertation). University of Birmingham.

Kadereit, G., Borsch, T., Weising, K., & Freitag, H. (2003). Phylogeny of Amaranthaceae and Chenopodiaceae and the evolution of C4 photosynthesis. *International Journal of Plant Sciences*, *164*(6), 959–986. https://doi.org/10.1086/378649

Kender, S., Stephenson, M. H., Riding, J. B., Leng, M. J., Knox, R. W. B., Peck, V. L., et al. (2012). Marine and terrestrial environmental changes in NW Europe preceding carbon release at the Paleocene-Eocene transition. *Earth and Planetary Science Letters*, *353*, 108–120. https://doi.org/10.1016/j.epsl.2012.08.011

Kim, J. S., & Kim, J. H. (2018). Updated molecular phylogenetic analysis, dating and biogeographical history of the lily family (Liliaceae: Liliales). *Botanical Journal of the Linnean Society*, *187*(4), 579–593. https://doi.org/10.1093/botlinnean/boy031

Lavin, M., Herendeen, P. S., & Wojciechowski, M. F. (2005). Evolutionary rates analysis of Leguminosae implicates a rapid diversification of lineages during the Tertiary. *Systematic Biology*, *54*(4), 575–594. https://doi.org/10.1080/10635150590947131

Leffingwell, H. A. (1970). Palynology of the Lance (Late Cretaceous) and Fort Union (Paleocene) Formations of the type Lance area, Wyoming. *Geological Society of America Special Papers*, *127*, 1–64.

Lehtonen, S. (2009). Systematics of the Alismataceae—A morphological evaluation. *Aquatic Botany*, *91*(4), 279–290. https://doi.org/10.1016/j.aquabot.2009.08.002

Levin, R. A., Wagner, W. L., Hoch, P. C., Nepokroeff, M., Pires, J. C., Zimmer, E. A., & Sytsma, K. J. (2003). Family-level relationships of Onagraceae based on chloroplast rbcL and ndhF data. *American Journal of Botany*, *90*(1), 107–115. https://doi.org/10.3732/ajb.90.1.107

Lindström, S., & Erlström, M. (2006). The late Rhaetian transgression in southern Sweden: Regional (and global) recognition and relation to the Triassic-Jurassic boundary. *Palaeogeography, Palaeoclimatology, Palaeoecology*, *241*(3-4), 339–372. https://doi.org/10.1016/j.palaeo.2006.04.006

Macphail, M. K., Alley, N. F., Truswell, E. M., & Sluiter, I. R. K. (1994). Early Tertiary vegetation: Evidence from spores and pollen. In R. S.Hill (Ed.), *History of the Australian vegetation: Cretaceous to recent* (pp. 189–261). Cambridge University Press.

Macphail, M. K., & Hill, R. S. (2019). What was the vegetation in northwest Australia during the Paleogene, 66–23 million years ago? *Australian Journal of Botany*, *66*(7), 556–574. https://doi.org/10.1071/BT18143

Manchester, S. R., & Chen, Z. D. (1998). A new genus of Coryloideae (Betulaceae) from the Paleocene of North America. *International Journal of Plant Sciences*, *159*(3), 522–532. https://doi.org/10.1086/297569

Mandel, J. R., Dikow, R. B., Siniscalchi, C. M., Thapa, R., Watson, L. E., & Funk, V. A. (2019). A fully resolved backbone phylogeny reveals numerous dispersals and explosive diversifications throughout the history of Asteraceae. *Proceedings of the National Academy of Sciences*, *116*(28), 14083–14088. https://doi.org/10.1073/pnas.1903871116

Mariani, E. (2019). Paleocene-Eocene Thermal Maximum oceanographic and vegetation changes. Presented at the AASP—The Palynological Society Conference, Ghent, Belgium.

McNeil, D. H., Parsons, M. G., & Russel-Houston, J. (2013). The Paleocene-Eocene thermal maximum in the Arctic Beaufort-Mackenzie Basin—Palynomorphs, carbon isotopes and benthic foraminiferal turnover. *Bulletin of Canadian Petroleum Geology*, *61*(2), 157–186. https://doi.org/10.2113/gscpgbull.61.2.157

Methner, K., Lenz, O., Riegel, W., Wilde, V., & Mulch, A. (2019). Paleoenvironmental response of midlatitudinal wetlands to Paleocene-early Eocene climate change (Schöningen lignite deposits, Germany). *Climate of the Past*, *15*(5), 1741–1755. https://doi.org/10.5194/cp-15-1741-2019

Mitchell, T. C., Williams, B. R., Wood, J. R., Harris, D. J., Scotland, R. W., & Carine, M. A. (2016). How the temperate world was colonised by bindweeds: Biogeography of the Convolvuleae (Convolvulaceae). *BMC Evolutionary Biology*, *16*(1), 1–12. https://doi.org/10.1186/s12862-016-0591-6

Moshayedi, M., Lenz, O. K., Wilde, V., & Hinderer, M. (2018). Controls on sedimentation and vegetation in an Eocene pull-apart basin (Prinz von Hessen, Germany): Evidence from palynology. *Journal of the Geological Society*, *175*(5), 757–773. https://doi.org/10.1144/jgs2017-128

Muller, J. (1981). Fossil pollen records of extant angiosperms. *The Botanical Review*, *47*(1), 1–142. https://doi.org/10.1007/BF02860537

Nichols, D. J. (1973). North American and European species of *Momipites* ("*Engelhardtia*") and related genera. *Geoscience and Man*, *7*(1), 103–117. https://doi.org/10.1080/00721395.1973.9989740

Nichols, D. J. (2010). *Reevaluation of the holotypes of the Wodehouse pollen species from the Green River Formation (Eocene, Colorado and Utah)*. American Association of Stratigraphic Palynologists Foundation.
Nichols, D. J., Ames, H. T., & Traverse, A. (1973). On *Arecipites* Wodehouse, *Monocolpopollenites* Thomson & Pflug, and the species "*Monocolpopollenites tranquillus*". *Taxon*, *22*(2-3), 241–256. https://doi.org/10.2307/1218131
Nichols, D. J., & Brown, J. L. (1992). *Palynostratigraphy of the Tullock Member (lower Paleocene) of the Fort Union Formation in the Powder River Basin, Montana and Wyoming*. U.S. Geological Survey Bulletin 1917-F. US Government Printing Office.
Nichols, D. J., & Ott, H. L. (1978). Biostratigraphy and evolution of the *Momipites-Caryapollenites* lineage in the early Tertiary in the Wind River Basin, Wyoming. *Palynology*, *2*(1), 93–112.
Pew, C. R. (2014). *The Paleocene Eocene Thermal Maximum in the Hanna Basin, WY: Constraints from organic carbon isotopes and palynological data* (Master's Dissertation). University of Washington.
Pocknall, D. T., & Nichols, D. J. (1996). *Palynology of coal zones of the Tongue River Member (upper Paleocene) of the Fort Union Formation, Powder River Basin, Montana and Wyoming (No. 32)*. American Association of Stratigraphic Palynologists Foundation.
Pole, M. (2010). Ecology of Paleocene-Eocene vegetation at Kakahu, South Canterbury, New Zealand. *Palaeontologia Electronica*, *13*(2), 29.
Prasad, V., Utescher, T., Sharma, A., Singh, I. B., Garg, R., Gogoi, B., et al. (2018). Low-latitude vegetation and climate dynamics at the Paleocene-Eocene transition—A study based on multiple proxies from the Jathang section in northeastern India. *Palaeogeography, Palaeoclimatology, Palaeoecology*, *497*, 139–156. https://doi.org/10.1016/j.palaeo.2018.02.013
Quesnel, F., Storme, J. Y., Roche, E., Iakovleva, A., Missiaen, P., Smith, T., et al. (2014). An unexpected record of the PETM in terrestrial and organic sediments of Avesnois, between the Paris and Belgian Basins, NW Europe (pp. 183–184). Presented at Climate and Biotic Events of the Paleogene: Ferrara, 1–6 July 2014.
Raine, J. I. (2008). Zonate lycophyte spores from New Zealand Cretaceous to Paleogene strata. *Alcheringa*, *32*(2), 99–127. https://doi.org/10.1080/03115510801916440
Raine, J. I., Mildenhall, D. C., & Kennedy, E. (2011). New Zealand fossil spores and pollen: An illustrated catalogue. *GNS Science Miscellaneous Series*, *4*(4).
Romero, I. C., Urban, M. A., & Punyasena, S. W. (2020). Airyscan superresolution microscopy: A high-throughput alternative to electron microscopy for the visualization and analysis of fossil pollen. *Review of Palaeobotany and Palynology*, *276*, 104192. https://doi.org/10.1016/j.revpalbo.2020.104192
Schmitz, B., Pujalte, V., & Nunez-Betelu, K. (2001). Climate and sea-level perturbations during the Incipient Eocene Thermal Maximum: Evidence from siliciclastic units in the Basque Basin (Ermua, Zumaia and Trabakua Pass), northern Spain. *Palaeogeography, Palaeoclimatology, Palaeoecology*, *165*(3-4), 299–320. https://doi.org/10.1016/S0031-0182(00)00167-X
Schuettpelz, E., Schneider, H., Huiet, L., Windham, M. D., & Pryer, K. M. (2007). A molecular phylogeny of the fern family Pteridaceae: Assessing overall relationships and the affinities of previously unsampled genera. *Molecular Phylogenetics and Evolution*, *44*(3), 1172–1185. https://doi.org/10.1016/j.ympev.2007.04.011
Shcherbinina, E., Gavrilov, Y., Iakovleva, A., Pokrovsky, B., Golovanova, O., & Aleksandrova, G. (2016). Environmental dynamics during the Paleocene-Eocene thermal maximum (PETM) in the northeastern Peri-Tethys revealed by high-resolution micropalaeontological and geochemical studies of a Caucasian key section. *Palaeogeography, Palaeoclimatology, Palaeoecology*, *456*, 60–81. https://doi.org/10.1016/j.palaeo.2016.05.006
Sluijs, A., Bijl, P. K., Schouten, S., Röhl, U., Reichart, G. J., & Brinkhuis, H. (2011). Southern Ocean warming, sea level and hydrological change during the Paleocene-Eocene thermal maximum. *Climate of the Past*, *7*(1), 47–61. https://doi.org/10.5194/cp-7-47-2011
Sluijs, A., Schouten, S., Donders, T. H., Schoon, P. L., Röhl, U., Reichart, G. J., et al. (2009). Warm and wet conditions in the Arctic region during Eocene Thermal Maximum 2. *Nature Geoscience*, *2*(11), 777–780. https://doi.org/10.1038/ngeo668
Sluijs, A., Schouten, S., Pagani, M., Woltering, M., Brinkhuis, H., Damsté, J. S. S., et al. (2006). Subtropical Arctic Ocean temperatures during the Palaeocene/Eocene thermal maximum. *Nature*, *441*(7093), 610–613. https://doi.org/10.1038/nature04668
Sluijs, A., Van Roij, L., Harrington, G. J., Schouten, S., Sessa, J. A., LeVay, L. J., et al. (2014). Warming, euxinia and sea level rise during the Paleocene-Eocene Thermal Maximum on the Gulf Coastal Plain: Implications for ocean oxygenation and nutrient cycling. *Climate of the Past*, *10*(4), 1421–1439. https://doi.org/10.5194/cp-10-1421-2014
Smith, V., Warny, S., Jarzen, D. M., Demchuk, T., Vajda, V., & Expedition 364 Science Party. (2020). Palaeocene-Eocene miospores from the Chicxulub impact crater, Mexico. Part 1: Spores and gymnosperm pollen. *Palynology*, *44*(3), 473–487. https://doi.org/10.1080/01916122.2019.1630860
Smith, V., Warny, S., Jarzen, D. M., Demchuk, T., Vajda, V., & Gulick, S. P. (2020). Paleocene-Eocene palynomorphs from the Chicxulub impact crater, Mexico. Part 2: Angiosperm pollen. *Palynology*, *44*(3), 489–519. https://doi.org/10.1080/01916122.2019.1705417
Soreng, R. J., Peterson, P. M., Romaschenko, K., Davidse, G., Zuloaga, F. O., Judziewicz, E. J., et al. (2015). A worldwide phylogenetic classification of the Poaceae (Gramineae). *Journal of Systematics and Evolution*, *53*(2), 117–137. https://doi.org/10.1111/jse.12150
Srivastava, S. K. (1972). Some spores and pollen from the Paleocene Oak Hill member of the Naheola Formation, Alabama (USA). *Review of Palaeobotany and Palynology*, *14*(3-4), 217–285. https://doi.org/10.1016/0034-6667(72)90021-8
Steurbaut, E., Magioncalda, R., Dupuis, C., Van Simaeys, S., Roche, E., & Roche, M. (2003). Palynology, paleoenvironments, and organic carbon isotope evolution in lagoonal Paleocene-Eocene boundary settings in North Belgium. *Geological Society of America Special Papers*, *369*, 291–317.
Suan, G., Popescu, S. M., Suc, J. P., Schnyder, J., Fauquette, S., Baudin, F., et al. (2017). Subtropical climate conditions and mangrove growth in Arctic Siberia during the early Eocene. *Geology*, *45*(6), 539–542. https://doi.org/10.1130/G38547.1
Sundue, M. A., Parris, B. S., Ranker, T. A., Smith, A. R., Fujimoto, E. L., Zamora-Crosby, D., et al. (2014). Global phylogeny and biogeography of grammitid ferns (Polypodiaceae). *Molecular Phylogenetics and Evolution*, *81*, 195–206. https://doi.org/10.1016/j.ympev.2014.08.017
Thornhill, A. H., Popple, L. W., Carter, R. J., Ho, S. Y., & Crisp, M. D. (2012). Are pollen fossils useful for calibrating relaxed molecular clock dating of phylogenies? A comparative study using Myrtaceae. *Molecular Phylogenetics and Evolution*, *63*(1), 15–27. https://doi.org/10.1016/j.ympev.2011.12.003
Traverse, A. (1994). Palynofloral geochronology of the Brandon Lignite of Vermont, USA. *Review of Palaeobotany and Palynology*, *82*(3-4), 265–297. https://doi.org/10.1016/0034-6667(94)90080-9
Wallander, E., & Albert, V. A. (2000). Phylogeny and classification of Oleaceae based on rps16 and trnL-F sequence data. *American Journal of Botany*, *87*(12), 1827–1841. https://doi.org/10.2307/2656836
Webster, G. L. (1994). Classification of the Euphorbiaceae. *Annals of the Missouri Botanical Garden*, 3–32. https://doi.org/10.2307/2399908
Willard, D. A., Donders, T. H., Reichgelt, T., Greenwood, D. R., Sangiorgi, F., Peterse, F., et al. (2019). Arctic vegetation, temperature, and hydrology during Early Eocene transient global warming events. *Global and Planetary Change*, *178*, 139–152. https://doi.org/10.1016/j.gloplacha.2019.04.012

Willard, D. A., Reichgelt, T., Greenwood, D. R., Robinson, M. M., & Self-Trail, J. M. (2019). Pollen-based reconstruction of Paleocene-Eocene climate in the mid-Atlantic region. Presented at AGU Fall Meeting Abstracts (PP31E-1681).

Willard, D. A., Robinson, M. M., Self-Trail, J. M., Wandless, G. A., & Sluijs, A. (2014). Pollen and palynofacies analyses of Paleocene-Eocene Thermal Maximum sediments from the North American continental shelf. Presented at AGU Fall Meeting Abstracts (PP11A-1331).

Willumsen, P. S., Schultz, B. P., & Sylvester, R. (2014). Rapid warming at the PETM and its influence on vegetation in Denmark. In P. S.Wilumsen, B. P.Schultz, & R.Sylvester (Eds.), *STRATI 2013* (pp. 159–162). Cham: *Springer*.

Wing, S. L., Harrington, G. J., Bowen, G. J., & Koch, P. L. (2003). Floral change during the Initial Eocene Thermal Maximum in the Powder River Basin, Wyoming. In S. L.Wing, P. D.Gingerich, B.Schmitz, & E.Thomas (Eds.), *Causes and consequences of globally warm climates in the early Paleogene* (Vol. 369, pp. 425–440). Boulder, Colorado: Geological Society of America Special Paper.

Wing, S. L., Harrington, G. J., Smith, F. A., Bloch, J. I., Boyer, D. M., & Freeman, K. H. (2005). Transient floral change and rapid global warming at the Paleocene-Eocene boundary. *Science*, *310*(5750), 993–996. https://doi.org/10.1126/science.1116913

Wodehouse, R. P. (1933). Tertiary pollen-II. The oil shales of the Eocene Green River formation. *Bulletin of the Torrey Botanical Club*, 479–524.

Worobiec, E., Widera, M., Worobiec, G., & Kurdziel, B. (2021). Middle Miocene palynoflora from the Adamów lignite deposit, central Poland. *Palynology*, *45*(1), 59–71. https://doi.org/10.1080/01916122.2019.1697388

Worobiec, E., Worobiec, G., & Gedl, P. (2009). Occurrence of fossil bamboo pollen and a fungal conidium of *Tetraploa* cf. *aristata* in Upper Miocene deposits of Józefina (Poland). *Review of Palaeobotany and Palynology*, *157*(3-4), 211–217. https://doi.org/10.1016/j.revpalbo.2009.05.002

Zetter, R., Farabee, M. J., Pigg, K. B., Manchester, S. R., DeVore, M. L., & Nowak, M. D. (2011). Palynoflora of the late Paleocene silicified shale at Almont, North Dakota, USA. *Palynology*, *35*(2), 179–211. https://doi.org/10.1080/01916122.2010.501164

Zhai, W., Duan, X., Zhang, R., Guo, C., Li, L., Xu, G., et al. (2019). Chloroplast genomic data provide new and robust insights into the phylogeny and evolution of the Ranunculaceae. *Molecular Phylogenetics and Evolution*, *135*, 12–21. https://doi.org/10.1016/j.ympev.2019.02.024